Directional formation of microtubes by soft-template electropolymerization from fully conjugated triphenylamine-based monomers

Khady Diouf, Abdoulaye Dramé, Alioune Diouf, François Orange, Frédéric Guittard, Igor F Perepichka, Thierry Darmanin

Directional formation of microtubes by soft-template electropolymerization from fully conjugated triphenylamine-based monomers

Khady Diouf [a], Abdoulaye Dramé[a], Alioune Diouf[a], François Orange[b], Frédéric Guittard[c], Igor F. Perepichka,[d,e,*] and Thierry Darmanin[c,*]

[a]*Université Cheikh Anta Diop, Faculté des Sciences et Techniques, Département de Chimie, B.P. 5005 Dakar, Sénégal*

[b]*Université Côte d'Azur, Centre Commun de Microscopie Appliquée (CCMA), 06100 Nice, France.*

[c]*Université Côte d'Azur, NICE Lab, 06100 Nice, France*

[d] *Department of Physical Chemistry and Technology of Polymers, Faculty of Chemistry, Silesian University of Technology, M. Strzody 9, Gliwice 44-100, Poland*

[e] *Centre for Organic and Nanohybrid Electronics, Silesian University of Technology, Konarskiego 22b, Gliwice 44-100, Poland*

* Corresponding author.

E-mail address: Thierry.darmanin@univ-cotedazur.fr (T. Darmanin);

i.perepichka@bangor.ac.uk (I. F. Perepichka)

ABSTRACT

Microtubular structures have been prepared by soft-template electropolymerization of conjugated organic monomers with the aim to mimic the strong water-adhesive forces of gecko foot or rose petals. Water-saturated solvent of low water solubility (dichloromethane) was used to form a micellar solution stabilized by tetrabutylammonium perchlorate as the electrolyte and the surfactant, in which case the formation of nanotubes was particularly efficient. The studied monomers were built from a triphenylamine core conjugated with three arms differing by their structure and positions: (i) 2- or 3-positions in the thiophene arms or (ii) carbazole arms attached to *para*, *meta* or *ortho*-positions of the benzene ring of the core. The formation of microtubes is due to preferential growth of polymer films and an aggregation of formed polymers/oligolymers in one direction (1D) facilitated by π–stacking interactions. The key factors influencing on the surface morphologies (monomer structures and reactivity, electrodeposition conditions, etc) are discussed. Impressive results have been obtained in

studies of carbazole-containing monomers and the effect of regioisomerism in the monomers (the position of the carbazole attachment to the core). Extremely long microtubes (tens to >100 μm length, diameter ≈ 1.0 – 1.5 μm) were formed on the electrode surface from the monomer **N-Ph-p-Cb** with the carbazole attachment in the *para*-position. Wettability analysis showed highly hydrophobic surfaces with apparent contact angles up to 154.0 ° and extremely strong water adhesion comparable to rose petals or gecko feet. Such coatings can find applications in water-harvesting systems, sensing platforms or electrochemical analyses.

Keywords: Adhesion, Conjugated polymers, Electropolymerization, Hydrophobicity, Surface structures, Triphenylamine, Thiophene, Carbazole, Regioisomerism.

1. Introduction

The control of surface structures at the nanoscale or microscale is fundamental for a huge number of applications such as in sensors, optics, catalysis, energy systems, biomaterials, cell culture [1,2,3,4], electrochemical analyses [5,6] or in wetting properties [7,8]. In nature, there are numerous species displaying extremely high hydrophobicity but also different water adhesive forces, such as lotus leaves, rose petals or gecko feet [9,10,11,12]. These surface wetting properties are highly dependent on both the surface energy and surface structures/features [13,14,15]. Different features were already investigated but the nanotubes are excellent candidates for their high surface area-to-volume ratio [16,17,18]. Jiang *et al.* also demonstrated stronger water adhesive forces compared to surfaces structures without pores [16].

There are few methods for forming well-defined nanotubes on a substrate. The electropolymerization is a very fast process while the tuning of non-porous structures (for instance nanofibers, nanosheets, nanospheres) is possible by changing the monomer or the electrochemical conditions [19]. Porous structures (for instance, nanotubes) are conceivable by electropolymerization on hard templates [20]. However, one hard template is necessary for each change in the nanotubes dimension (diameter, height or pitch). One of the most used hard templates are Anodic Aluminum Oxide (AAO) membranes but these membranes have to be removed after use. Strategies without hard templates are called templateless or soft-template electropolymerization. The soft template can be composed of gas bubbles or micelles in solution. When the electropolymerization is performed in water (H_2O), oxygen (O_2) bubbles can be produced on the electrode during electropolymerization because the potential of H_2O and the monomer oxidation potential are close [21,22,23,24,25]. Porous structures can be produced if the polymer growth around these gas bubbles. It is also possible to

produce hydrogen (H_2) bubbles by reducing H_2O using potentiodynamic electropolymerization such as cyclic voltammetry (CV) or pulse deposition. Most of the monomers are not soluble in H_2O, and low polarity solvents such as dichloromethane (CH_2Cl_2) or chloroform ($CHCl_3$) can be used as soon as trace H_2O is present in solution [26,27,28,29]. The process is completely different because micelles can be present in solution prior electropolymerization [27]. Micelles can be formed in solution if the electrolyte and/or the monomer play the role of a surfactant thus stabilizing these micelles. They will wet the substrate before electropolymerization.

To construct nanotubes on a substrate by electropolymerization, it is necessary to favor the polymerization in one direction (1D growth) [30]. The molecular structures that can induce strong π–stacking interactions, such as 3,4-(1,2-naphthylenedioxy)thiophene (NaphDOT) [26, 27], 3,4-phenylenedioxythiophenes (PheDOTs) [31,32,33] and some others [28], demonstrated exceptional preliminary results. The polymerization rate should not be also too fast because the 1D growth takes time as demonstrated by reducing the temperature [34]. Another proof of the importance of electropolymerization rate was demonstrated by comparing the surfaces obtained by electrodeposition of substituted PheDOT monomer and its dimer [31]. Whereas the monomer formed nice vertically aligned nanotubes, the dimer gave 3-dimensional spherical nanoparticles. The monomer and polymer solubilities are also important parameters influencing the process of electrodeposition [35,36,37]. The research group of Wang investigated tris(4-(thien-2-yl)phenyl)amine (Chart 1, **N-Ph-2-Th**) as promising molecule for the formation of tubular structures by soft-template electropolymerization in similar electrochemical conditions [38]. Other cores (tetraphenylmethane, 9,9′-spirobifluorene) were also tested [39,40,41], while the effect of water on the electropolymerization and surface morphology was not investigated.

In this work, we have synthesized and investigated electropolymerization and the surface properties of electrodeposited films for two series of conjugated molecules based on the triphenylamine core differing by the fashion of the thiophene (2- or 3-positions, **N-Ph-2-Th** and **N-Ph-3-Th**) or carbazole arms attachment (*para- / meta- / ortho-*, **N-Ph-p-Cb**, **N-Ph-m-Cb**, **N-Ph-o-Cb**) (Chart 1). The monomers of high polymerization capacity (thiophene derivatives) and lower polymerization capacity (carbazole derivatives) were chosen. We studied the influence of the monomer structure, the effect of water presence in the solution during the electropolymerization, as well as the electrodeposition method on the resulting surface structures. The presence of reverse micelles was studied by transmission electron microscopy (TEM), the polymer films formation was investigated by cyclic voltammetry, and the surface structures was analyzed by scanning electron microscopy (SEM) and the surface wettability by goniometry.

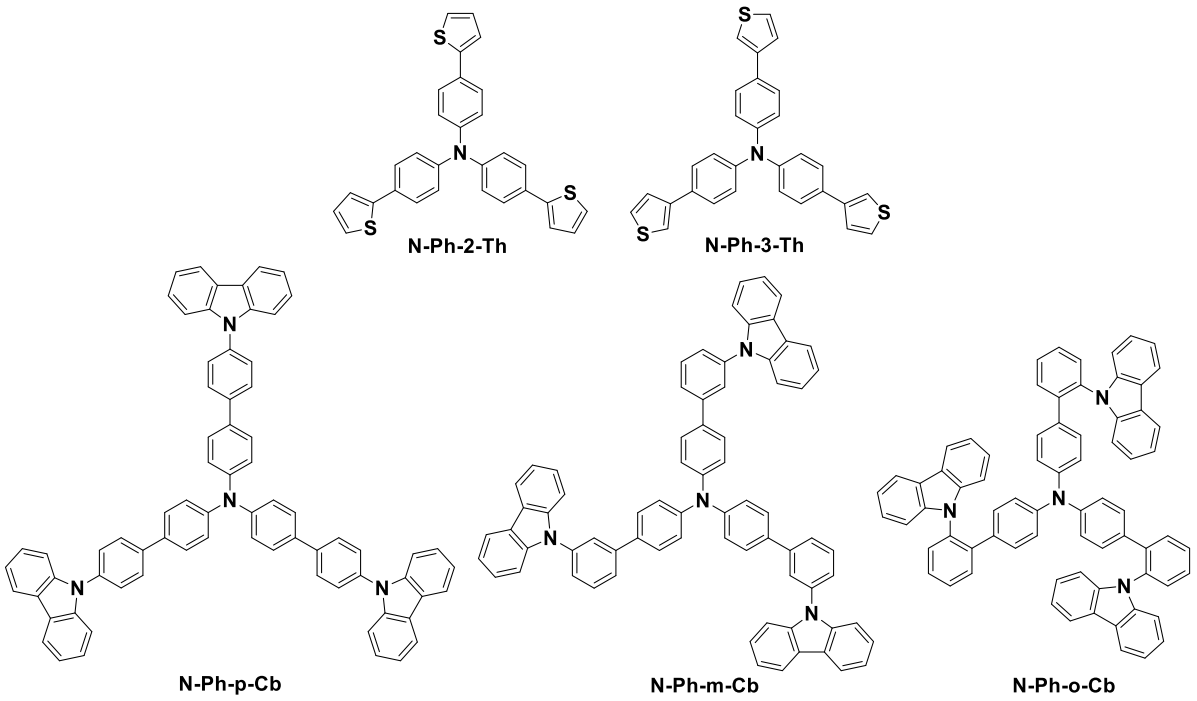

Chart 1. Structures of monomers investigated by soft-template electropolymerization.

2. Results and discussion

2.1. Synthesis of monomers

Synthesis and characterization of monomers shown in Chart 1 have been presented in the Supporting Information (SI). Briefly, synthesis was done by Pd(0)-catalyzed Suzuki coupling of tris(4-bromophenyl)amine with corresponding arylboronic acids (Scheme S1, SI), and the products were purified by column chromatography.

2.2 DFT computational studies

The geometry and electronic structures of monomers were studied computationally by DFT method at the B3LYP/6-31G(d) level of theory. The optimized geometries of the monomers are shown in Figure S1, and the key dihedral angles between the conjugated fragments in the structures are presented in Table 1. The molecules are not flat because steric hindrances result in some distortion between the conjugated units. The dihedral angles at the central triphenylamine core (~ 41 °) and between the benzene rings and thiophene (26–30 °) or carbazole moieties (~ 55 °) are typical connections between these units. An exception is **N-Ph-o-Cb**, in which case large steric hindrance of *ortho*-substitution with carbazole moiety significantly distorts the structure and increases the dihedrals angles to 67.3 – 70.8 ° (Table 1).

Table 1. Key dihedral angles between the moieties in the studied monomers.[a]

Compound	Ph-N-Ph (°)	Ph-Th (°)	Ph-Ph (°)	Ph-Cb (°)
N-Ph-2-Th	41.0	25.7		
N-Ph-3-Th	41.1	30.1		
N-Ph-p-Cb	41.1		35.3	54.8
N-Ph-m-Cb	41.0		35.6	56.5
N-Ph-o-Cb[b]	38.7 / 42.4		46.0 / 48.1	70.8 / 67.3

[a] Ph-N-Ph are dihedrals in the central triphenylamine core; Ph-Th are dihedrals between the benzene and thiophene rings; Ph-Ph are dihedrals between benzene rings of the biphenyl fragment; Ph-Cb are dihedrals between the benzene and carbazole rings. [b] Bulky carbazole moiety in *ortho*-position in **N-Ph-o-Cb** results in different dihedral angles measured at different sides of the moieties.

Yet, one should consider that in conjugated polymers derived from these monomers, an extended conjugation and solid-state packing can make these building blocks a bit flatter. The effect should be the most pronounced in the case of **N-Ph-2-Th** due to extension of the conjugation length when coupling at the positions 5 of the thiophene rings occurs (producing fragment "N–Ph–Th–Th–Ph–N") and slightly smaller in **N-Ph-3-Th**. Electropolymerization of carbazole derivatives is known to occur at positions 3,6. Because carbazole rings significantly distorted from the triphenylamine plane, growing the polymer chains (especially for **N-Ph-o-Cb**) will likely occur near orthogonally to the triphenylamine plane (or, at least, far away from the extension along the triphenylamine plane).

The energies of the highest occupied molecular orbitals (HOMOs) and lowest unoccupied molecular orbitals (LUMOs) of the studied compounds together with HOMOs and LUMOs for thiophene, carbazole and triphenylamine molecules are given in Figure 1. It is seen that HOMO energies of studied compounds are close to that in triphenylamine, indicating significant contribution of the core. In contrast, substantial lowering their LUMOs (compared to Th, Cb or Ph3N building blocks) reflects an extension of the conjugation.

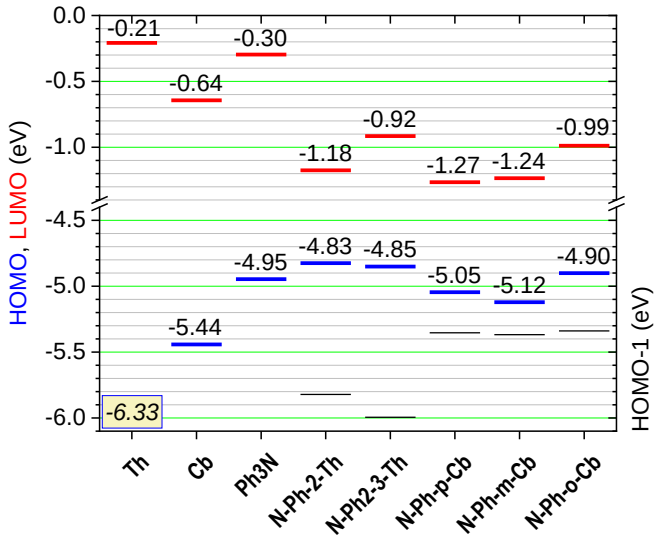

Figure 1. Frontier orbitals energy levels of studied monomers and subunits used in their structures.

Figure 2 shows delocalization of HOMOs and LUMOs in the molecules. HOMOs are mainly delocalized over the triphenylamine core, but with significant extension to the end thiophene rings in the arms (for **N-Ph-2Th** and **N-Ph-3-Th**) or (at less extent) to carbazole moieties in the case of para-substituted **N-Ph-p-Cb**. HOMO orbital coefficients on carbazole moieties in **N-Ph-p-Cb** are small and are negligible in **N-Ph-m-Cb** and **N-Ph-o-Cb**, while lower energy levels (HOMO-1 to HOMO-3) sit on the carbazole moieties (Figure S2 in the SI; see also Figure 2 for HOMO-1 energies). LUMO orbitals also mainly sits on the triphenylamine core, extending to peripheral thiophene or phenylene moieties (Figure 1; keep in mind the degeneracy of the orbitals due to the C_3-symmetry of the studied molecules).

These results indicate that triphenylamine core should be significantly involved in the initial electron transfer process (oxidation) to form radical cations species during the electropolymerization process. Really, calculations of electronic structures of radical cation species from these molecules (intermediates in anodic electropolymerization process) at spin-unrestricted UB3LYP/6-31G(d) level of theory show significant spin delocalization over the central triphenylamine core with an extension to thiophene and carbazole end groups (Figure 3). As expected, in the arms, the largest spin coefficients are observed at positions 2,5 for the thiophene moieties and 3,6 for the carbazole moieties.

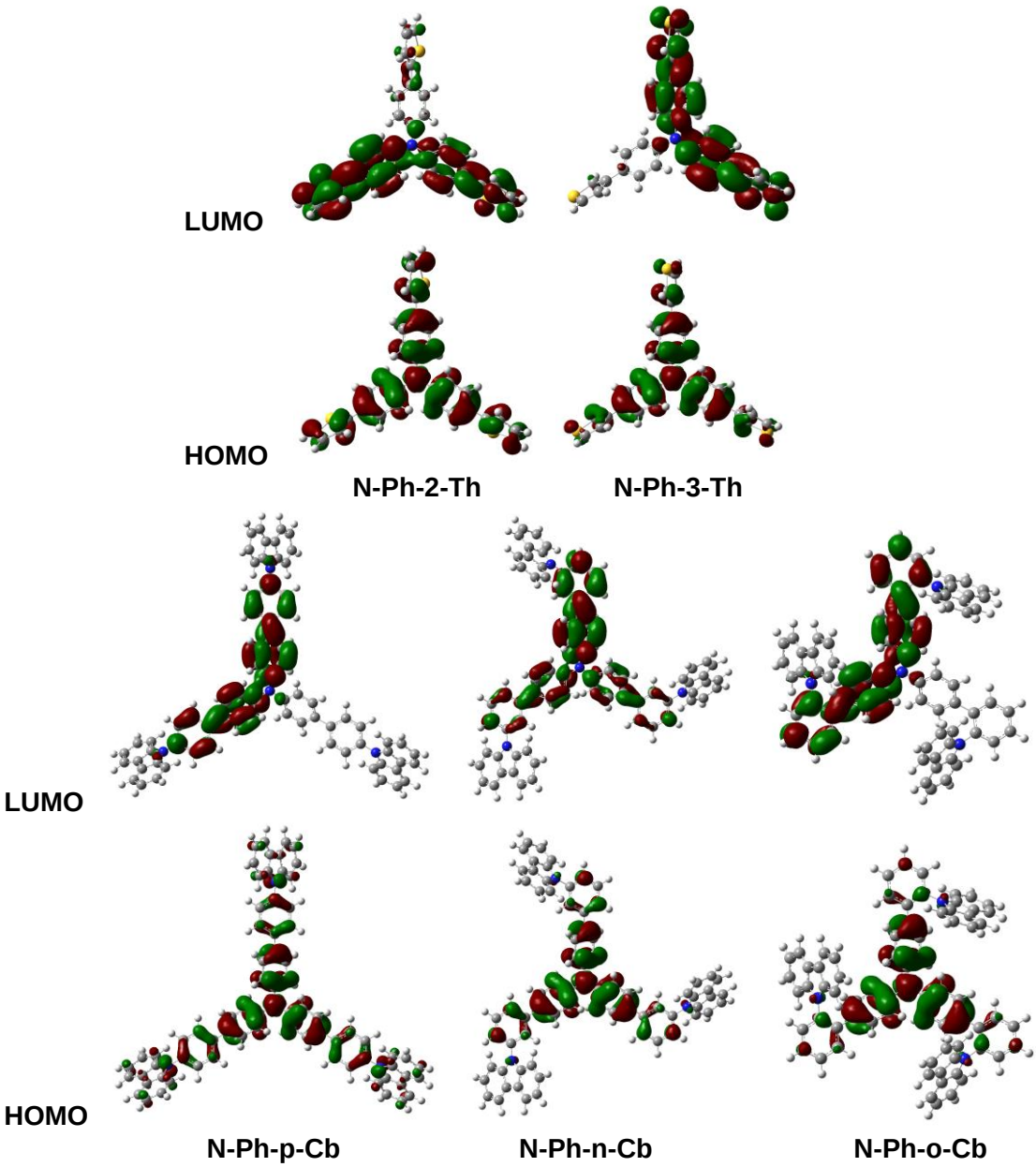

Figure 2. Frontier orbital coefficients distribution in studied monomers from DFT calculations at B3LYP/6-31G(d) level.

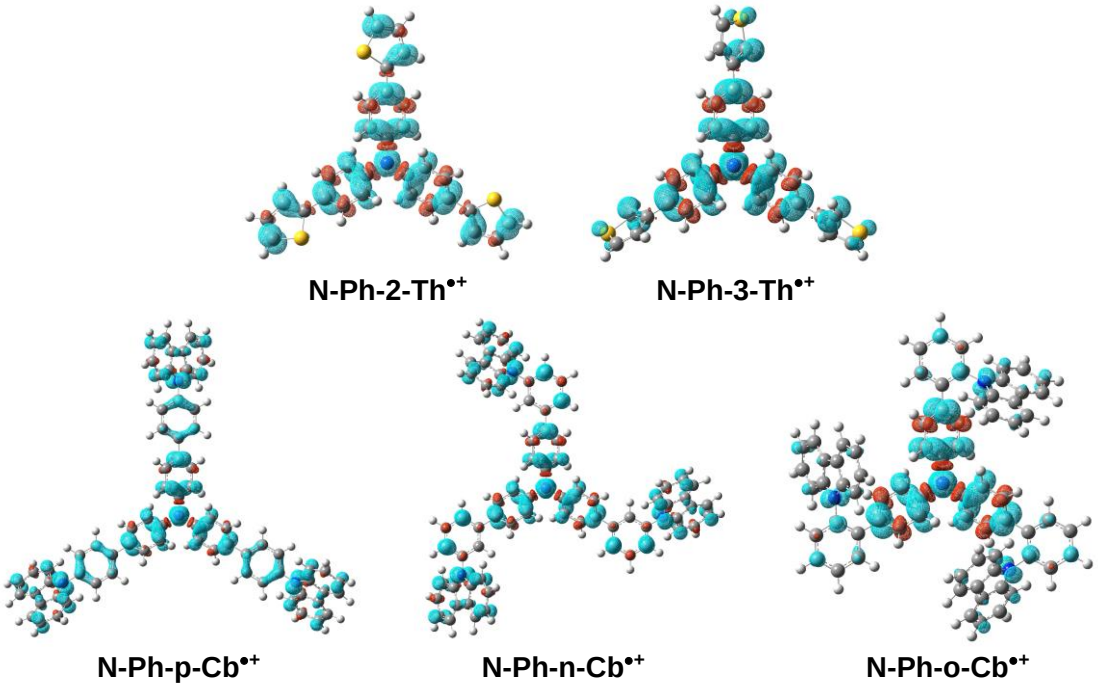

Figure 3. Spin density maps for radical cations of studied monomers, calculated at UB3LYP/6-31G(d) level in a gas phase. The cyan color surface corresponds to an excess of α-electron density and the red surface (negative spin density) corresponds to an excess of β-electron density. The isosurface value is 0.001.

2.3. Electrochemical deposition of polymer films from monomers onto the electrode surface

The polymer films were electrodeposited on gold-coated silicon wafer electrode by electropolymerization of monomers (0.005 M) in two solvents, i.e. dichloromethane (CH_2Cl_2) and dichloromethane saturated with water (CH_2Cl_2 + H_2O sat.), with 0.1 M of Bu_4NClO_4 as an electrolyte. Both potentiodynamic (by cyclic voltammetry) and potentiostatic deposition techniques were used.

As shown below, micellar solutions were produced by mixing (CH_2Cl_2 + H_2O sat.) with the electrolyte tetrabutylammonium perchlorate (Bu_4NClO_4). We previously studied electropolymerization of another monomer, NaphDOT, in CH_2Cl_2 and (CH_2Cl_2 + H_2O sat.) with Bu_4NClO_4 as an electrolyte and found a relationship between the size of micelles formed in solution prior electropolymerization (by transmission electron microscopy, TEM) and the size of the resulting nanotubes formed on the surface (by SEM) [27]. While we tested many tetrabutylammonium salts with different counter anions, i.e. perchlorate (ClO_4^-), tetrafluoroborate (BF_4^-), hexafluorophosphate (PF_6^-), trifluoromethanesulfonate ($CF_3SO_3^-$), perfluorobutanesulfonate ($C_4F_9SO_3^-$), perfluorooctanesulfonate ($C_8F_{17}SO_3^-$), and bis(trifluoromethane) sulfonimide (Tf_2N^-), nanotubes were formed only with ClO_4^- and BF_4^- [42]. Tetrabutylammonium perchlorate is not a typical amphiphilic surfactant having high critical micelle concentration values in water (CMC > 0.25 M) [43], and we did not investigate the influence of electrolyte concentration. Here, to confirm the

presence of micelles in the monomer solutions in Bu_4NClO_4 / (CH_2Cl_2 + H_2O sat.) prior electropolymerization, they have been studied by TEM. The obtained TEM images clearly demonstrate the formation of micelles of different sizes for different monomers (Figure 4).

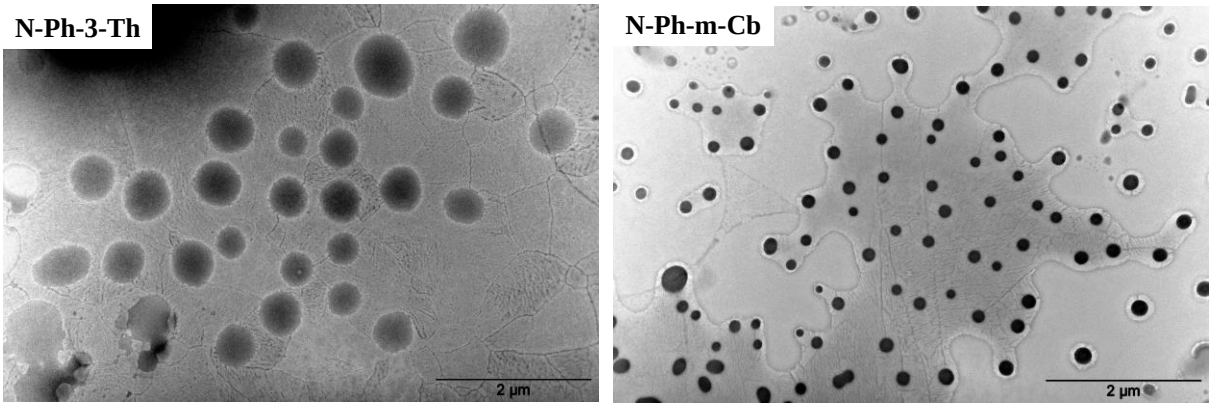

Figure 4. TEM images of **N-Ph-3-Th** and **N-Ph-m-Cb** (0.005 M) in (CH_2Cl_2 + H_2O sat.) with 0.1 M of Bu_4NClO_4.

(CH_2Cl_2 + H_2O sat.) solvent was also tested toward producing O_2 and/or H_2 gas bubbles from H_2O during the electropolymerization ($2H_2O \rightarrow O_2 + 4H^+ + 4e^-$; $2H_2O + 2e^- \rightarrow H_2 + 2OH^-$). Water oxidation potential lies in the range of oxidation potentials of studied monomers, while water reduction is close to –0.5 V. This means that H_2 bubbles can only be produced by potentiodynamic polymerization such as cyclic voltammetry (CV) or pulse deposition. Therefore, the effect of two different deposition methods, i.e. potentiodynamic (by CV) and potentiostatic (at constant potential) electropolymerization, have been tested.

Our proposed mechanism of vesicle/tube formation is as follows. The studied monomers are insoluble in H_2O, but soluble in CH_2Cl_2. In (CH_2Cl_2 + H_2O sat.) solution and in the presence of Bu_4NClO_4, inverse micelles (i.e. with H_2O inside the micelles) are formed and dispersed in CH_2Cl_2. Bu_4NClO_4 is an electrolyte soluble in CH_2Cl_2 but because it is a surfactant, it is present in large quantities at the CH_2Cl_2/H_2O interface. When the working electrode (here is gold) is inserted in solution, micelles will wet the substrate following the Young's theory: liquid (H_2O)/liquid (CH_2Cl_2)/solid (gold) interface. During electropolymerization, the electrodeposited polymer will grow from the substrate but only in the parts in contact to CH_2Cl_2 due to the absence of monomer in H_2O. On applied potential for redox process, H_2O present on the substrate is transformed into gas bubbles. O_2 bubbles are formed at constant (positive) potential and both O_2 and H_2 are formed in CV experiments. These bubbles also participate in the formation of specific surface structure. For the formation of nanotubes, it is important that the polymer grows in one direction.

First, the monomer oxidation potentials (E^{ox}) were determined by fast CV scans between 0 and 2.5 V *vs* SCE (Figure 5). For studied monomers, one or two intense peaks were observed in the potential range of ≈ 1.7 – 2.5 V. For E^{ox}, we took the first intense peaks at E^{ox} = 1.75 – 2.00 V *vs* SCE (their E^{onset} ≈ 1.2 – 1.4 V). Therefore, the electrodeposition of polymer films was performed at the first intense oxidation peaks (≈ 1.7 V) with each monomer giving thick films deposition at these potentials. We should also mention that the other oxidation peaks of much smaller intensitities were also observed for all monomers at lower potentials of ≈ 1 V *vs* SCE. These peaks correspond well to oxidation potentials of triphenylamine and its derivatives [44,45] and belong to the 1e oxidation of triphenylamine core in the monomers.

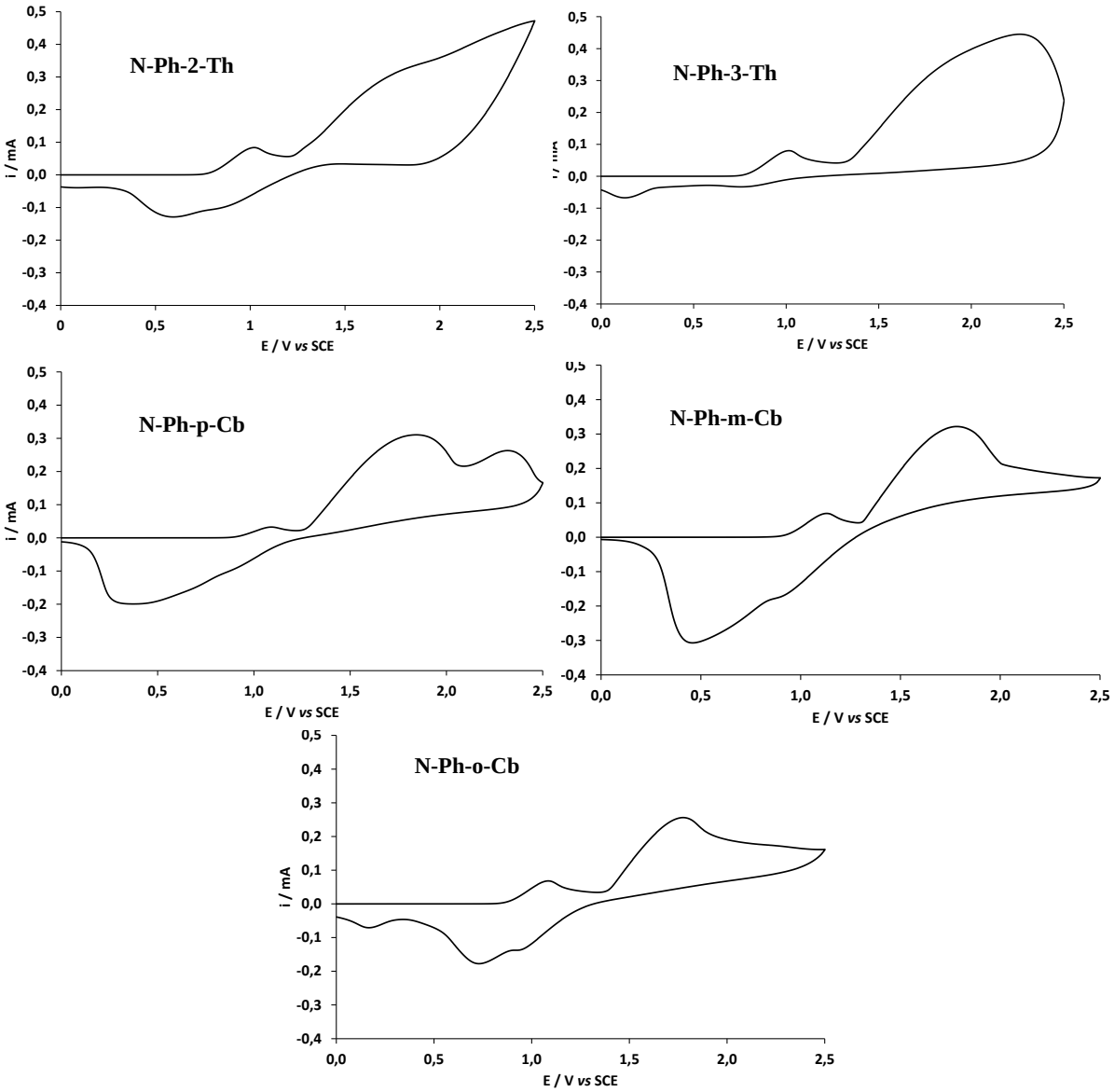

Figure 5. Cyclic voltammograms of studied monomers in CH_2Cl_2 with 0.1 M of Bu_4NClO_4. The potential range sweep is from 0 to 2.5 V, scan rate is 100 mV s^{-1}. The first scans are shown.

Polymer films were electrodeposited by CV scanning in the range from –1 V to E^{ox} in order to release a large number of gas bubbles (Figure S3 in the SI). A scan rate of 20 mV s^{-1} was used, as well as different numbers of deposition scans (1, 3, or 5 scans). The obtained films were then electrochemically characterized by CV in monomer-free solutions of 0.1 M Bu_4NClO_4 / CH_2Cl_2 (Figure 6).

All electrodeposited films show p-doping electrochemical response of several poorly resolved/overlapped peaks/shoulders in the range of ca. 1 – 2 V, i.e. close to that for starting monomers. This contrasts with the usual behavior of 1D conjugated polymers prepared by electropolymerization method (e.g. polythiophenes, polypyrroles, polyfluorenes etc) whose electroactivity is generally observed at significantly lower potentials than that for corresponding monomers. This difference can be explained by the fact that the conjugation length of the whole molecules is not increased significantly on coupling at the thiophene or carbazole sites.

The exception is polymerization of **N-Ph-2-Cb**, electrochemical coupling of which produces an extended conjugation in the fragment "N–Ph–Th–Th–Ph–N". This is particularly reflected by an appearance of an additional wave at low potential of ≈ 0.64 V (i.e. lower than that for triphenylamine oxidation in the monomer), which distinguishes it from other electrodepositions (Figure 6). For **N-Ph-3-Th** and carbazole-containing monomers (**N-Ph-p-Cb**, **N-Ph-m-Cb** and **N-Ph-p-Cb**), coupling of monomers only slightly increases the conjugation at coupled Th–Th or Cb–Cb fragments. It should also be taken into account that the used monomers are crowded trifunctional molecules of C_3 symmetry (see DFT section 2.2), so their electropolymerization can be stopped (or retarded) at the stage of rather short oligomers due to steric issues. Such oligomers, due to their low solubility, can aggregate and deposit on the surface. Thus, we have recently demonstrated that NaphDOT derivatives functionalized at position 2 of the thiophene ring (to prevent electropolymerization with the formation of conjugated polymers) form only dimers in CV experiments, which, due to their low solubility, are deposited on the surface forming growing unidirectional (1D) vertically aligned nanotubes, likely due to good π-π stacking of flat dimers [32].

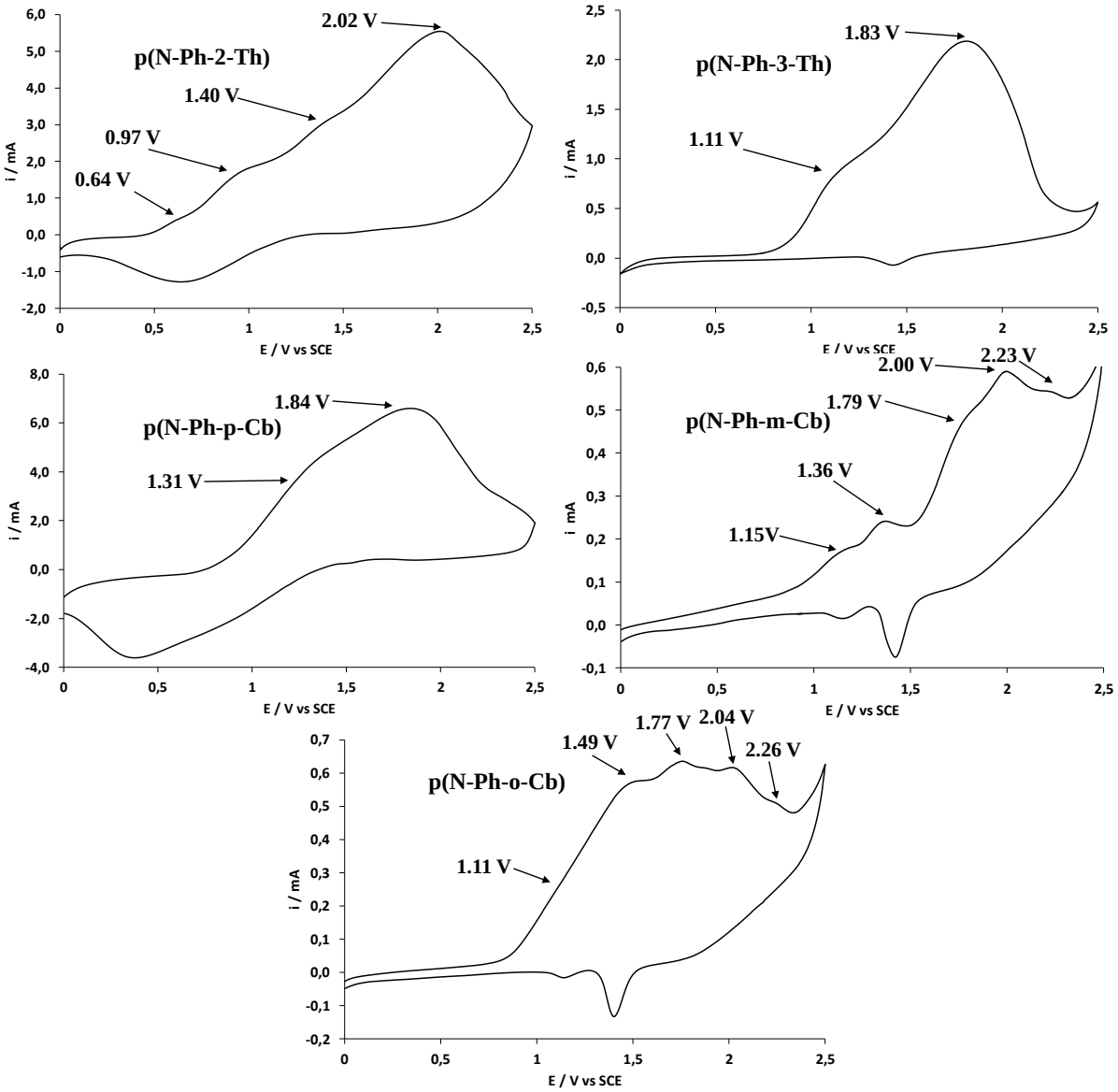

Figure 6. Cyclic voltammograms of electrodeposited polymers in monomer-free solutions of CH_2Cl_2 with 0.1 M of Bu_4NClO_4. The polymers were obtained by potendiodynamic polymerization (5 cycles) scanning from 0 to 2.5 V at the scan rate 20 mV s^{-1}.

2.4. Surface morphology and nanostructures

In CH_2Cl_2, the surfaces made from **N-Ph-2-Th** and **N-Ph-p-Cb** are extremely rough, but only non-porous cauliflower-like structures are observed, which means a classical three-dimension (3D) growth (Figure 7). However, some tubules (apart of spherical, likely hollow, structures) are present in the films made from **N-Ph-3-Th**, showing a higher capacity to form tubular structures due to preferential growth in one direction. The formation of porous structures in CH_2Cl_2 with increased number of tubules is possible if trace H_2O is present in solution.

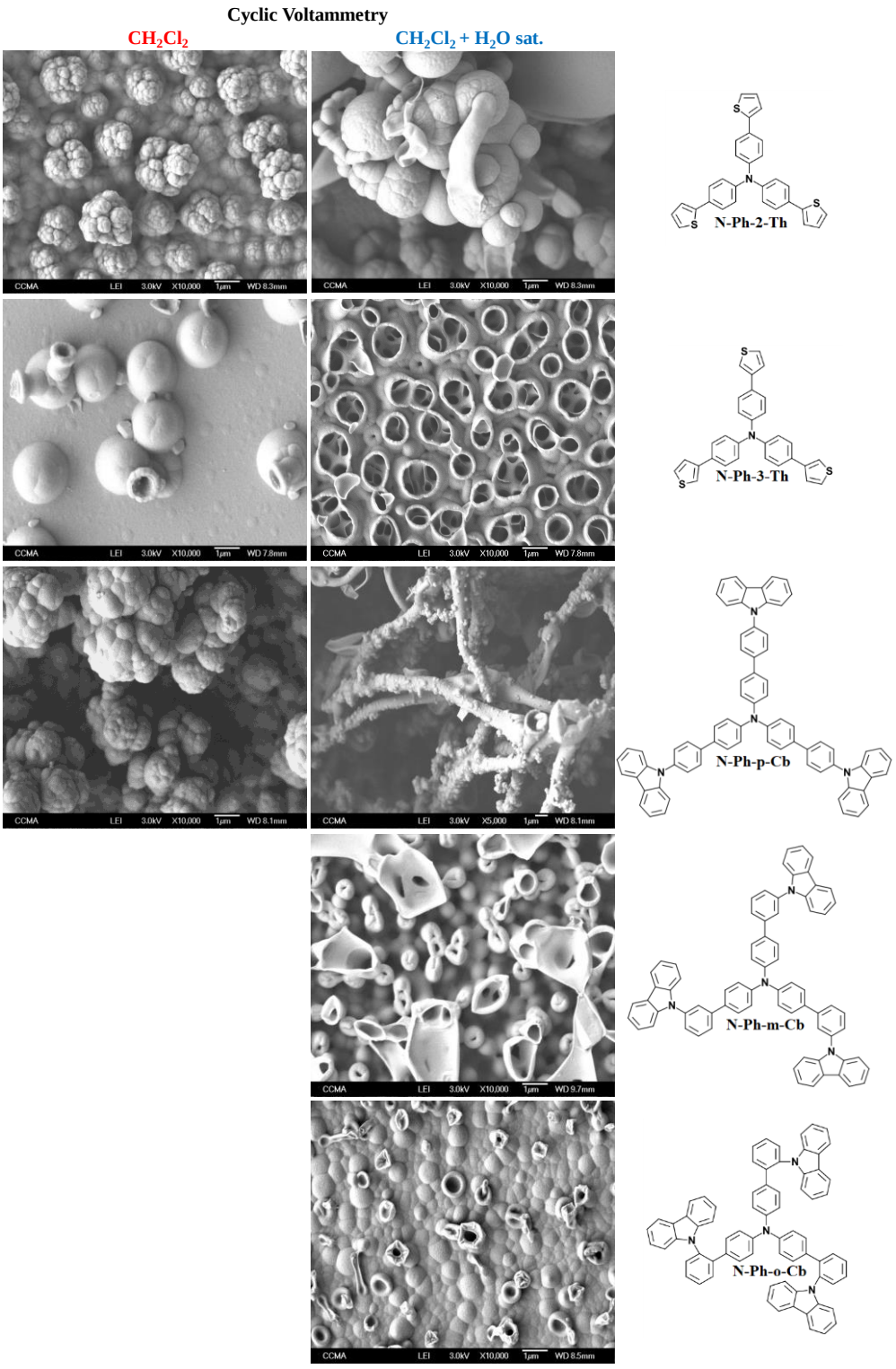

Figure 7. SEM images of electrodeposited surfaces from each monomer by CV. The modified surfaces were obtained in CH_2Cl_2 or (CH_2Cl_2 + H_2O sat.) with 0.1 M of Bu_4NClO_4 for 3 scans in the potential range from –1 V to E^{ox} at the scan rate 20 mV s^{-1}. Magnification is ×10,000 (×5,000 for **N-Ph-p-Cb** in (CH_2Cl_2 + H_2O sat.)).

Therefore, more detailed studies have been performed in (CH_2Cl_2 + H_2O sat.) (Figure 7, right column). In the case of **N-Ph-2-Th**, both cauliflower-like structures and microtubes are formed, while in the case of **N-Ph-3-Th** densely -packed microtubes of a large diameter (≈ 0.5 – 1 μm) are observed. Such densely packed microtubules from **N-Ph-3-Th** are formed already after 1 scan, and with increasing the number of scans, the height of the tubes increases while the top of the tubes becomes close (Figure S4 in the SI). In the case of carbazole-containing monomers (**N-Ph-p-Cb**, **N-Ph-m-Cb**, and **N-Ph-o-Cb**), microtubular structures are formed for all regioisomers, but the position of carbazole attachment to the terminal benzene ring of the core (*para*-, *meta*-, or *ortho*-) has a huge impact on the resulting surface structures. These significant differences are even better seen from the SEM images with inclination angles of 45° (Figure 8).

The most impressive surface structures are observed for the compound with the carbazole moiety in *para*-position (**N-Ph-p-Cb**). In this case, ultra-long tubes (≈ 1.0 – 1.5 μm in diameterwith tens to >100 μm length) are growing, indicating the preferential polymer growth / packing along one direction (1D), although the formed tubes are not aligned along the single axis but form disordered wool-like / fiber-like high-surface structure. Better flatness of **N-Ph-p-Cb** (compared to **N-Ph-m-Cb** and **N-Ph-o-Cb**; Figure S1 in the SI) and less steric hindrance for coupling at both 3- and 6- positions of the carbazole moieties promote faster electropolymerization and the formation of more ordered structures, likely through some kind of π–stacking of deposited oligomers/polymers in a direction perpendicular to the triphenylamine plane, resulting in extremely long tubular structures. These results are in line with previous work on comparative electropolymerization of 3,4-phenylenedioxythiphenes with 1-naphthyl or 2-naphthyl groups in the side chain (1Na-PheDOT and 2Na-PheDOT, respectively) [31]. Electropolymerization of 1Na-PheDOT, which has smaller steric hindranes from naphtyl groups (according to B3LYP/6-31G(d) studies of optimized geometries) gave uniform, vertically aligned nanotubes, whereas 2Na-PheDOT electrodeposition gave disordered nanoribbons. In the case of **N-Ph-m-Cb**, a two-step process of the surface development is observed. Initially (one CV scan), densely packed and almost uniformly vertically oriented microtubes are formed. The mean diameter of the tubes is rather small (≈ 350 – 500 nm) and most of the tubes have their top close. As the number of scans increases, large-diameter (≈ 1.5 – 5 μm) open spheres (tulip-like structures) are formed on the top of the tubes. In the case of **N-Ph-o-Cb**, the most sterically crowded monomer, the number of tubes is significantly less. After 1 scan, the surface structure mainly consist of hemi-spheres and rings (diameter ≈ 1 μm), while after 5 scans, cups of large diameter are formed (diameter ≈ 1.5 – 3 μm, height ≈ 1.5 – 2 μm).)

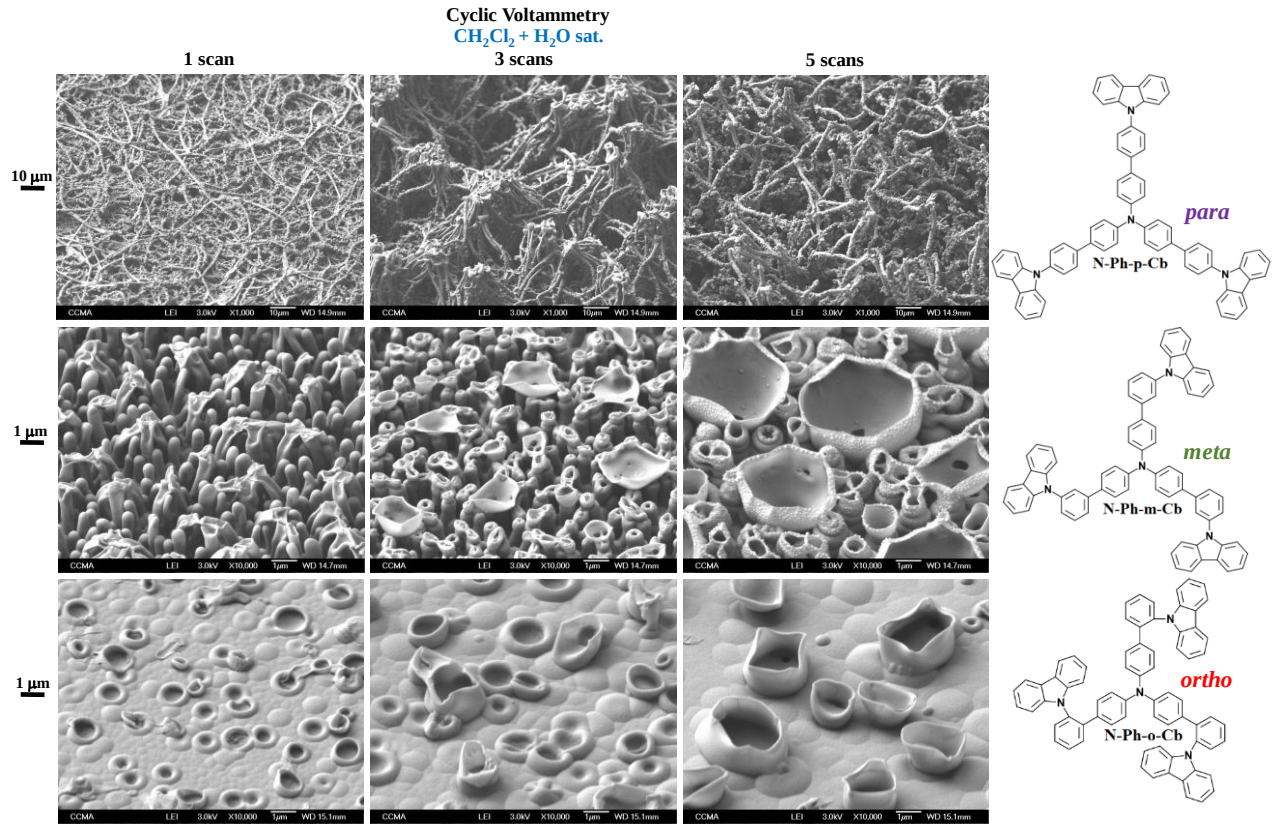

Figure 8. SEM images with an inclination angle of 45 ° of potentiodynamically (CV) electrodeposited surfaces from **N-Ph-p-Cb**, **N-Ph-m-Cb** and **N-Ph-o-Cb** by CV for 1, 3 and 5 scans. The modified surfaces were obtained in (CH_2Cl_2 + H_2O sat.) with 0.1 M of Bu_4NClO_4 by scanning in the potential range from –1 V to E^{ox} at the scan rate 20 mV s^{-1}. Magnifications are ×1,000, ×10,000 and ×10,000, respectively.

We also performed depositions under potentiostatic conditions at constant potential $E = E^{ox}$ (1.75 – 2.00 V, depending on the monomer) to investigate the effect of the deposition method (current-time curves are shown in Figure S5 in the SI). In these conditions, only O_2 bubbles are produced from H_2O ($2H_2O \rightarrow O_2 + 4H^+ + 4e^-$). The experiments were performed varying the deposition charges (12.5, 25, 50, 100, 200, 400 mC cm^{-2}), and SEM images of surfaces prepared at 100 mC cm^{-2} are shown in Figure 9. Here, the structures obtained at constant potential are relatively close to that obtained by CV method, but often at high deposition charges. For example, ultra-long and mostly horizontally oriented nanofibers have been observed with **N-Ph-p-Cb** in (CH_2Cl_2 + H_2O sat.), but only at a deposition charge of 400 mC cm^{-2}.

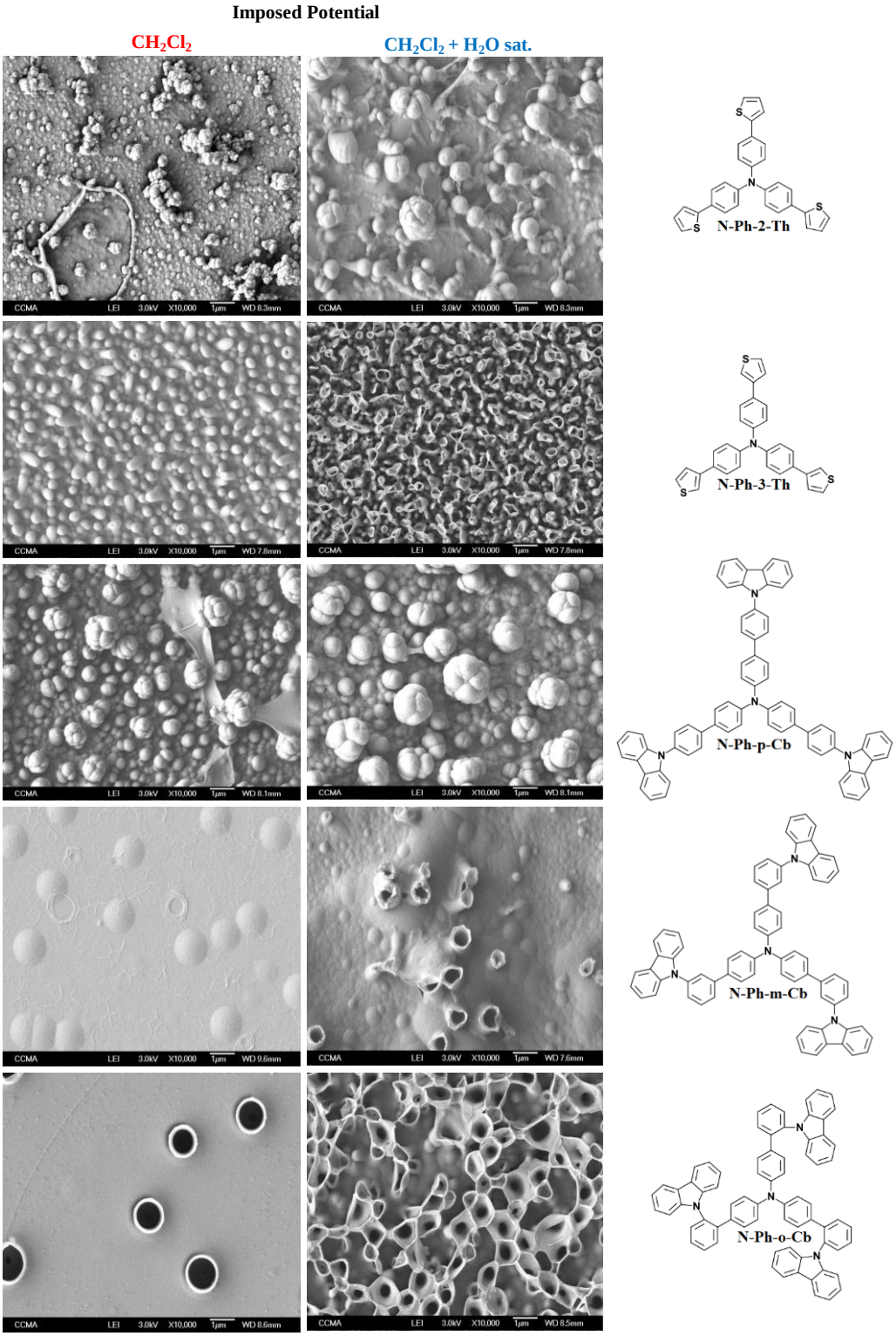

Figure 9. SEM images of potentiostatically electrodeposited surfaces from each monomer at constant potential of E^{ox}. The modified surfaces were obtained in CH_2Cl_2 or (CH_2Cl_2 + H_2O sat.) with 0.1 M of Bu_4NClO_4 at the deposition charge of 100 mC cm^{-2}. Magnification is ×10,000.

2.5 Surface wettability

The wettability of all surfaces, electrodeposited from studied monomers in both solvents, CH_2Cl_2 and (CH_2Cl_2 + H_2O sat.), was also studied (Table 2). To better evaluate the effect of surface roughness, smooth surfaces have also been prepared (see SI for the details) to obtain the Young's contact angles (θ^Y) [46] and surface energy (γ_{SV}) [47] of each polymer (Table 3). The most intrinsically hydrophilic surface is that derived from **N-Ph-2-Th** (θ^Y_w = 60.5 °) while the only intrinsically hydrophobic surface (θ^Y_w > 90 °) is the surface derived from **N-Ph-p-Cb**.

The results obtained with **N-Ph-2-Th** in (CH_2Cl_2 + H_2O sat.) are impressive (θ_w up to 154.0 °, Table 2), especially considering that this is the most hydrophilic polymer (θ^Y_w = 60.5 °, Table 3), and are due to the presence of both cauliflower-like structures and nanotubes. This transition from hydrophilic to hydrophobic state can only be explained by the Cassie-Baxter equation (1) [48] confirming the presence of an important air fraction between water droplet and the rough surface:

$$\cos \theta = r_f f \cdot \cos \theta^Y + f - 1 \quad (1)$$

where θ and θ^Y are apparent contact angles for rough and smooth surfaces, r_f is the roughness ratio of the substrate wetted by the liquid, f and (1 – f) are the solid and air fractions, respectively.

For densely packed large-diameter nanotubes obtained with **N-Ph-3-Th**, a maximum of θ^Y = 134.3 ° was achieved. Even larger maxima θ^Y = 150.7 ° and 146.8 ° were obtained for **N-Ph-p-Cb** and **N-Ph-m-Cb**, consisting of extremely long mostly horizontally oriented nanotubes and tulip-like structures, respectively. In the case of **N-Ph-o-Cb**, the surfaces are much less hydrophobic (θ_w up to 99.5 °) because their roughness is smaller. Moreover, these surfaces are also "sticky", like rose petals or gecko feet [12,49], so water droplets remain stuck on them whatever the tilting angle is.

As mentioned in the previous section, the structure/morphology of surfaces obtained in potentiostatic conditions at E^{ox} potentials is generally similar to (or not very different from) that obtained in potentiodynamic conditions by CV. However, the surfaces deposited under potentiostatic conditions are much more hydrophilic (θ_w < 100°; Table 4). Indeed, at a constant potential, the electrodeposited polymers are in the p-doped state, hence, with polar perchlorate (ClO_4^-) counterions, which should also increase surface energy.

Table 2. Apparent contact angles for rough dedoped polymer films prepared by CV electrodeposition.[a]

Monomer	Number of scans	Solvent: CH_2Cl_2			Solvent: (CH_2Cl_2 + H_2O sat.)		
		θ_w (°)	θ_{DIM} (°)	θ_{HD} (°)	θ_w (°)	θ_{DIM} (°)	θ_{HD} (°)
N-Ph-2-Th	1 scan	93.1	<10	<10	123.2	<10	<10
	3 scans	109.6	<10	<10	**154.0**	<10	<10
	5 scans	114.2	<10	<10	**151.4**	<10	<10
N-Ph-3-Th	1 scan	71.0	23.3	<10	63.3	49.4	<10
	3 scans	72.0	18.8	<10	132.9	11.8	<10
	5 scans	47.0	17.7	<10	134.3	13.9	<10
N-Ph-p-Cb	1 scan	143.0	16.3	<10	138.0	<10	<10
	3 scans	142.6	<10	<10	145.5	<10	<10
	5 scans	137.0	<10	<10	**150.7**	<10	<10
N-Ph-m-Cb	1 scans	X	X	X	146.8	<10	<10
	3 scans	X	X	X	144.3	14.1	<10
	5 scans	X	X	X	139.6	11.7	<10
N-Ph-o-Cb	1 scan	X	X	X	69.7	23.8	<10
	3 scans	X	X	X	77.3	15.8	<10
	5 scans	X	X	X	99.5	11.6	<10

[a] θ_w, θ_{DIM} and θ_{HD} are apparent contact angles of water, diiodomethane and hexadecane droplets, respectively, with the electrodeposited films surface.

Table 3. Apparent contact angles and surface energy for smooth dedoped polymer films.[a]

Monomer	θ^Y_w (°)	θ^Y_{DIM} (°)	θ^Y_{HD} (°)	γ_{SV}	$\gamma_{SV,D}$	$\gamma_{SV,P}$
N-Ph-2-Th	60.5	23.5	<10	47.6	31.4	16.2
N-Ph-3-Th	85.0	47.8	14.4	33.2	28.7	4.6
N-Ph-p-Cb	**94.2**	41.0	12.0	32.9	31.4	1.5
N-Ph-m-Cb	89.8	50.0	16.5	31.3	28.6	2.7
N-Ph-o-Cb	85.1	44.5	12.7	33.6	29.7	3.9

[a] θ^Y_w, θ^Y_{DIM} and θ^Y_{HD} are apparent contact angles (Young's angles) of water, diiodomethane and hexadecane droplets, respectively, with smooth film surfaces. [b] γ_{SV} surface tensions between a solid and a gas; D and V superscripts denote disperse (apolar) and polar parts of surface energies calculated by Owens-Wendt equation [47].

Table 4. Apparent contact angles for the rough p-doped polymer films prepared at constant potential E^{ox}.

Monomer	Deposition charge (mC cm^{-2})	Solvent: CH_2Cl_2 θ_w (°)	θ_{DIM} (°)	θ_{HD} (°)	Solvent: (CH_2Cl_2 + H_2O sat.) θ_w (°)	θ_{DIM} (°)	θ_{HD} (°)
N-Ph-2-Th	12.5	75.6	<10	<10	63.3	<10	<10
	25	72.5	<10	<10	60.4	<10	<10
	50	69.3	<10	<10	70.1	<10	<10
	100	75.8	<10	<10	90.7	<10	<10
	200	50.1	<10	<10	84.6	<10	<10
	400	59.4	<10	<10	69.8	<10	<10
N-Ph-3-Th	12.5	49.6	23.2	<10	76.7	22.7	<10
	25	42.3	13.2	<10	79.1	14.9	<10
	50	51.1	<10	<10	67.8	13.3	<10
	100	87.7	<10	<10	32.0	39.8	<10
	200	90.1	<10	<10	37.6	44.7	<10
	400	59.4	40.0	<10	43.1	62.1	<10
N-Ph-p-Cb	12.5	80.6	26.2	<10	66.0	22.1	<10
	25	54.2	31.4	<10	81.1	12.1	<10
	50	64.8	27.7	<10	72.9	25.5	<10
	100	55.5	<10	<10	55.7	17.9	<10
	200	64.3	<10	<10	71.4	12.4	<10
	400	67.6	<10	<10	60.0	<10	<10
N-Ph-m-Cb	12.5	63.1	27.0	<10	88.9	23.0	<10
	25	80.4	16.6	<10	93.2	21.1	<10
	50	76.2	23.6	<10	81.2	15.1	<10
	100	67.3	26.0	<10	79.7	18.3	<10
	200	84.9	24.4	<10	87.8	16.6	<10
	400	51.9	30.6	<10	82.5	21.1	<10
N-Ph-o-Cb	12.5	90.5	31.0	<10	80.7	25.4	<10
	25	79.1	26.0	<10	79.5	31.2	<10
	50	76.0	44.9	<10	81.1	26.9	<10
	100	60.1	45.7	<10	80.6	26.4	<10
	200	76.0	31.8	<10	71.3	20.4	<10
	400	98.5	29.4	<10	87.1	27.6	<10

3. Conclusion

In this article, we used a soft-template electropolymerization approach to form microtubules on the surface of a substrate from electropolymerizable conjugated monomers. Low water-solubility solvent (dichloromethane) was saturated with water to form a micellar solution stabilized by Bu_4NClO_4 as the electrolyte and the surfactant. Under these conditions (CH_2Cl_2 + H_2O sat.), the formation of nanotubes was especially straightforward process.

Two series of monomers composed of a triphenylamine core conjugated with thiophene (2- or 3-positions of thiophene attached to *para*-position of the benzene ring of triphenylamine) or carbazole arms (attached by its N atom to *para*-, *meta*- or *ortho*-positions of the benzene ring of the core) have been invewstigated. DFT calculations of the geometry and electronic structures (for both neutral and radical cation states) of the monomers have been performed to understand the coupling processes during the electropolymerization.

Except for the **N-Ph-2-Th** monomer (with attached 2-thiophene arms), coupling/electropolymerization of which extends the conjugation in the "N-Ph-Th-Th-Ph-N" fragment, resulting on lower oxidation potentials, oxidation potentials other monomers are comparable/overlapping with those for the monomers. The surface structures of the electrodeposited films are significantly influenced by the structure of the monomers, including the nature of the arms (thiophene or carbazole) and the regioisomerism (the place of an attachment of the arms), as well as the electrodeposition conditions. The formation of microtubes is induced by π-stacking interactions between the monomer moieties of polymer/oligomer chains during the electrodeposition, allowing a preferential growth in one direction (1D). Because the 1D growth takes time, the rate of the polymerization/deposition is also significant factor. Unique results have been demonstrated by simply changing the attachment position of the carbazole arms: in the case of the **N-Ph-p-Cb** monomer with carbazole arms in the *para*-position to the benzene ring of the triphenylamine ring, ultra-long microtubes were formed (tens to >100 μm length and diameter ≈ 1 – 1.5 μm). The extremely strong water-adhesive forces, comparable to gecko foot or rose petals, with very high $\theta_w > 150$ ° have been demonstrated for electrodeposited surfaces from **N-Ph-2-Th** and **N-Ph-p-Cb** in (CH_2Cl_2 + H_2O sat.). These results can be used in the future in a number of applications such as water-harvesting systems, electrochemical analysis or sensing platforms.

Declaration of Competing Interest

The authors declare that they have no known competing financial interests or personal relationships that could have appeared to influence the work reported in this paper.

Acknowledgement

The group thanks Christelle Boscagli from the Centre Commun de Microscopie Appliquée (CCMA, Université Côte d'Azur) for the preparation of the substrates necessary for the SEM analyses. This work was supported by CNRS GDR 2088 « BIOMIM ». IFP acknowledges EU's Horizon 2020 ERA-Chair project ExCEED (grant agreement No. 952008).

Supplementary data

Supporting Information to this article is available online at https://doi.org/10.1016/j.jelechem.XXX and contains: used materials and instruments, synthesis and characterization of monomers and their ^{1}H / ^{13}C NMR copies, computational methodology and Cartesian coordinates of optimized geometries, methods of electropolymerization and surface characterizations.

References

[1] C.Y. Xu, J.L. Li, X.Y. Feng, J.W. Zhao, C.J. Tang, B.M. Ji, J. Hu, C.B. Cao, Y.Q. Zhu, F.K. Butt, The improved performance of spinel $LiMn_2O_4$ cathode with micro-nanostructured sphere-interconnected-tube morphology and surface orientation at extreme conditions for lithium-ion batteries, Electrochim. Acta 358 (2020) 136901.

[2] S. Ai, G. Lu, Q. He, J. Li, Highly flexible polyelectrolyte nanotubes, J. Am. Chem. Soc. 125 (2003) 11140–11141.

[3] V. Schroeder, S. Savagatrup, M. He, S. Lin, T.M. Swager, Carbon nanotube chemical sensors, Chem. Rev. 119 (2019) 599–663.

[4] D. Tasis, N. Tagmatarchis, A. Bianco, M. Prato, Chemistry of carbon nanotubes, Chem. Rev. 106 (2006) 1105–1136.

[5] E.W. McQueen, J.I. Goldsmith, Electrochemical analysis of single-walled carbon nanotubes functionalized with pyrene-pendant transition metal complexes, J. Am. Chem. Soc. 131 (2009) 17554–17556.

[6] E.E.S. Bruzaca, R.C. de Oliveira, M.S.S. Duarte, C.P. Sousa, S. Morais, A.N. Correia, P. de Lima-Neto, Electrochemical sensor based on multi-walled carbon nanotubes for imidacloprid determination, Anal. Methods 13 (2021) 2124–2136.

[7] T. Darmanin, F. Guittard, Molecular design of conductive polymers to modulate superoleophobic properties, J. Am. Chem. Soc. 131 (2009) 7928–7933.

[8] B. Su, Y. Tian, L. Jiang, Bioinspired interfaces with superwettability: From materials to chemistry, J. Am. Chem. Soc. 138 (2016) 1727–1748.

[9] W. Barthlott, C. Neinhuis, Purity of the sacred lotus, or escape from contamination in biological surfaces, Planta 202 (1997) 1–8.

[10] T. Darmanin, F. Guittard, Superhydrophobic and superoleophobic properties in nature, Mater. Today 18 (2015) 273–285.

[11] B. Bhushan, Bioinspired structured surfaces, Langmuir 28 (2012) 1698–1714.

[12] L. Feng, Y. Zhang, J. Xi, Y. Zhu, N. Wang, F. Xia, L. Jiang, Petal effect: A superhydrophobic state with high adhesive force, Langmuir 24 (2008) 4114–4119.

[13] M. Marmur, Wetting on hydrophobic rough surfaces: To be heterogeneous or not to be? Langmuir 19 (2003) 8343–8348.

[14] T. Tuteja, W. Choi, M. Ma, J.M. Mabry, S.A. Mazzella, G.C. Rutledge, G.H. McKinley, R. E. Cohen, Designing superoleophobic surfaces, Science 318 (2007) 1618–1622.

[15] C. Raufaste, G. Ramos Chagas, T. Darmanin, C. Claudet, F. Guittard, F. Celestini, Superpropulsion of droplets and soft elastic solids, Phys. Rev. Lett. 119 (2017) 108001.

[16] Z. Cheng, J. Gao, L. Jiang, Tip geometry controls adhesive states of superhydrophobic 6surfaces, Langmuir 26 (2010) 8233–8238.

[17] K.K.S. Lau, J. Bico, K.B.K. Teo, M. Chhowalla, G.A.J. Amaratunga, W.I. Milne, G.H. McKinley, K.K. Gleason, Superhydrophobic carbon nanotube forests, Nano Lett. 3 (2003) 1701–1705.

[18] Y.K. Lai, F. Pan, C. Xu, H. Fuchs, L.F. Chi, In situ surface-modification-induced superhydrophobic patterns with reversible wettability and adhesion, Adv. Mater. 25 (2013) 1682–1686.

[19] T. Darmanin, F. Guittard, Wettability of conducting polymers: From superhydrophilicity to superoleophobicity, Prog. Polym. Sci. 39 (2014) 656–682.

[20] H.-A. Lin, S.-C. Luo, B. Zhu, C. Chen, Y. Yamashita, H.-h. Yu, Molecular or nanoscale structures? The deciding factor of surface properties on functionalized poly(3,4-ethylenedioxythiophene) nanorod arrays, Adv. Funct. Mater. 23 (2013) 3212–3219.

[21] C. Debiemme-Chouvy, A. Fakhry, F. Pillier, Electrosynthesis of polypyrrole nano/micro structure using an electrogenerated oriented polypyrrole nanowire array as framework, Electrochim. Acta 268 (2018) 66–72.

[22] L. Qu, G. Shi, F. Chen, J. Zhang, Electrochemical growth of polypyrrole microcontainers, Macromolecules 36 (2003) 1063−1067.

[23] S. Gupta, Hydrogen bubble-assisted syntheses of polypyrrole micro/nanostructures usi.ng electrochemistry: Structural and physical property characterization, J. Raman Spectrosc. 39 (2008) 1343–1355.

[24] J.T. Kim, S.K. Seol, J.H. Je, Y. Hwu, G. Margaritondo, The microcontainer shape in electropolymerization on bubbles, Appl. Phys. Lett. 94 (2009) 034103.

[25] M. Wysocka-Zołopa, K. Winkler, Electrochemical synthesis and properties of conical polypyrrole structures, Electrochim. Acta 258 (2017) 1421–1434.

[26] T. Darmanin, F. Guittard, A one-step electrodeposition of homogeneous and vertically aligned nanotubes with parahydrophobic properties (high water adhesion), J. Mater. Chem. A 4 (2016) 3197–3203.

[27] C. Fradin, F. Orange, S. Amigoni, C.R. Szczepanski, F. Guittard, T. Darmanin, Micellar formation by soft template electropolymerization in organic solvents, J. Colloid Interface Sci. 590 (2021) 260–267.

[28] Y. Levieux-Souid, A. Sathanikan, F. Orange, F. Guittard, T. Darmanin, Densely packed open microspheres by soft template electropolymerization of benzotrithiophene-based monomers, Electrochim. Acta 369 (2021) 137677.

[29] D. Possetto, I. Pecnikaj, G. Marzari, S. Orlandi, S. Sereno, M. Cavazzini, G. Pozzi, F. Fungo, Influence of polyfluorinated side chains and soft-template method on the surface morphologies and hydrophobic properties of electrodeposited films from fluorene bridged dicarbazole monomers, ChemPhysChem 24 (2023) e202200371.

[30] Y.C. Zhao, J. Stejskald, J.X. Wang, Towards directional assembly of hierarchical structures: Aniline oligomers as the model precursors, Nanoscale 5 (2013) 2620–2626.

[31] T. Darmanin, E. L. Klimareva, I. Schewtschenko, F. Guittard, I.F. Perepichka, Exceptionally strong effect of small structural variations in functionalized 3,4-phenylenedioxythiophenes on

the surface nanostructure and parahydrophobic properties of their electropolymerized films, Macromolecules 52 (2019) 8088–8102

[32] C. Fradin, F. Guittard, I.F. Perepichka, T. Darmanin, Soft-template electropolymerization of 3,4-(2,3-naphtylenedioxy)thiophene-2-acetic acid esters favoring dimers: Controlling the surface nanostructure by side ester groups, Electrochim. Acta 425 (2022) 140684.

[33] T. Darmanin, G. Godeau, F. Guittard, E.L. Klimareva, I. Schewtschenko, I.F. Perepichka, A templateless electropolymerization approach to porous hydrophobic nanostructures using 3,4-phenylenedioxythiophene monomers with electron-withdrawing groups, ChemNanoMat 4 (2018) 656–662.

[34] S.-C. Luo, J. Sekine, B. Zhu, H. Zhao, A. Nakao, H.-h. Yu, Polydioxythiophene nanodots, nonowires, nano-networks, and tubular structures: The effect of functional groups and temperature in template-free electropolymerization, ACS Nano 6 (2012) 3018–3026.

[35] E. Poverenov, M. Li, A. Bitler, M. Bendikov, Major effect of electropolymerization solvent on morphology and electrochromic properties of PEDOT films, Chem. Mater. 22 (2010) 4019–4025.

[36] I.F. Perepichka, S. Roquet, P. Leriche, J.-M. Raimundo, P. Frère, J. Roncali, Electronic properties and reactivity of short-chain oligomers of 3,4-phenylenedioxythiophene (PheDOT), Chem. Eur. J. 12 (2006) 2960 – 2966.

[37] I.F. Perepichka, E. Levillain, J. Roncali, Effect of substitution of 3,4-ethylenedioxythiophene (EDOT) on the electronic properties of the derived electrogenerated low band gap conjugated polymers, J. Mater. Chem. 14 (2004) 1679–1681.

[38] S.L. Bai, Q. Hu, Q. Zeng, M. Wang, L.S. Wang, Variations in surface morphologies, properties, and electrochemical responses to nitro-analyte by controlled electropolymerization of thiophene derivatives, ACS Appl. Mater. Interfaces 10 (2018) 11319–11327.

[39] A. Palma-Cando, G. Brunklaus, U. Scherf, Thiophene-based microporous polymer networks via chemical or electrochemical oxidative coupling, Macromolecules 48 (2015) 6816–6824.

[40] I. Rendón-Enríquez, A. Palma-Cando, F. Körber, F. Niebisch, M. Forster, M.W. Tausch, U. Scherf, Thin polymer films by oxidative or reductive electropolymerization and their application in electrochromic windows and thin-film sensors, Molecules 28 (2023) 883.

[41] S. Napierała, M. Kubicki, V. Patroniak, M. Wałesa-Chorab, Electropolymerization of [2 × 2] grid-type cobalt(II) complex with thiophene substituted dihydrazone ligand, Electrochim. Acta 369 (2021) 137656.

[42] T. Darmanin, J.-P. Laugier, F. Orange, F. Guittard, Influence of the monomer structure and electrochemical parameters on the formation of nanotubes with parahydrophobic properties (high water adhesion) by a templateless electropolymerization process, J. Colloid Interface Sci. 466 (2016) 413–424.

[43] P. Saxena, Y. Singh, P. Jain, Thermodynamic parameters of quaternary ammonium salts TMAC, TEAB, TBAB and TBAI in aqueous and methanolic solutions at 298.16K, 303.16K, 308.16K and 313.16K by conductivity measurements, International Journal of Engineering Science and Computing 8 (2018) 18213. Available online at http://ijesc.org/

[44] J.M. Campina, Potentiostatic electropolymerization of triphenylamine: a low-cost cathode for solid-state photovoltaics, J. Electrochem. Soc. 162 (2015) H142–H150.

[45] P. Blanchard, C. Malacrida, C. Cabanetos, J. Roncali, S. Ludwigs, Triphenylamine and some of its derivatives as versatile building blocks for organic electronic applications, Polym. Int. 68 (2019) 589–606.

[46] T. Young, An essay on the cohesion of fluids, Philos. Trans. R. Soc. London 95 (1805) 65–87.

[47] D.K. Owens, R.C. Wendt, Estimation of the surface free energy of polymers, J. Appl. Poly. Sci. 13 (1969) 1741–1747.

[48] A.B.D. Cassie, S. Baxter, Wettability of porous surfaces, Trans. Faraday Soc. 40 (1944) 546–551.

[49] C.R. Szczepanski, T. Darmanin, F. Guittard, Recent advances in the study and design of parahydrophobic surfaces: From natural examples to synthetic approaches. Adv. Colloid Interface Sci. 241 (2017) 37–61.

Graphical Abstract

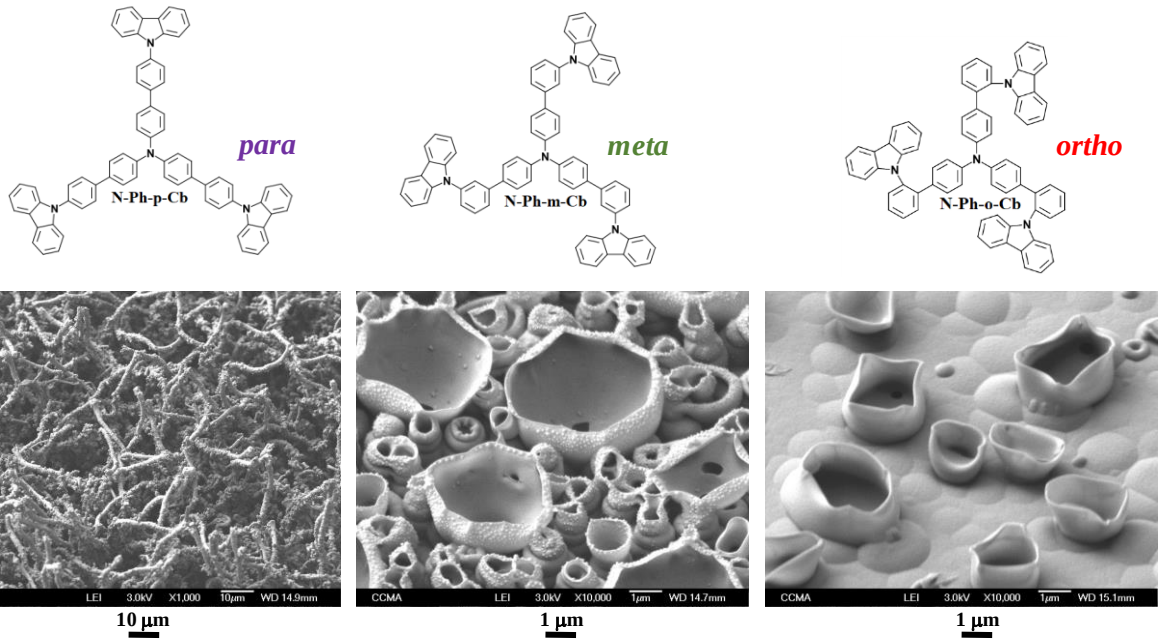

Supporting Information

Directional formation of microtubes by soft-template electropolymerization from fully conjugated triphenylamine-based monomers

Khady Diouf [a], Abdoulaye Dramé[a], Alioune Diouf[a], François Orange[b], Frédéric Guittard[c], Igor F. Perepichka,[d,e,*] and Thierry Darmanin[c,*]

[a]*Université Cheikh Anta Diop, Faculté des Sciences et Techniques, Département de Chimie, B.P. 5005 Dakar, Sénégal*

[b]*Université Côte d'Azur, Centre Commun de Microscopie Appliquée (CCMA), 06100 Nice, France.*

[c]*Université Côte d'Azur, NICE Lab, 06100 Nice, France*

[d] *Department of Physical Chemistry and Technology of Polymers, Faculty of Chemistry, Silesian University of Technology, M. Strzody 9, Gliwice 44-100, Poland*

[e] *Centre for Organic and Nanohybrid Electronics, Silesian University of Technology, Konarskiego 22b, Gliwice 44-100, Poland*

* Corresponding author.

E-mail address: Thierry.darmanin@univ-cotedazur.fr (T. Darmanin);
i.perepichka@bangor.ac.uk (I. F. Perepichka)

Experimental section

Monomer synthesis and characterization.

Tris(4-(thiophen-2-yl)phenyl)amine(**N-Ph-2-Th**) was purchased from Sigma Aldrich. Tris(4-bromophenyl)amine and all the used boronic acids were purchased from TCI. The other original monomers were synthesized from tris(4-bromophenyl)amine and by three Suzuki reactions as shown in Scheme S1. The components used for the Suzuki reaction were tris(4-bromophenyl)amine (2 mmol, 1.0 eq.), the corresponding boronic acid (7.0 mmol, 3.5 eq.), tetrakis(triphenylphosphine)-

palladium(0) (0.1 mmol, 0.1 eq.) and sodium carbonate (4.0 g). These components were mixed to a solution containing 100 mL of toluene, 20 mL of ethanol and 10 mL of water, and were refluxed for 3 days. After solvent evaporation, the crude products were purified by column chromatography (silica gel; eluent: petroleum ether).

NMR spectra were obtained with a 400 MHz ultra blinded spectrometer equipped with an AVANCE III Nano HD electronic console. The proton and carbon frequencies were 400.13MHz and 100.63MHz, respectively.

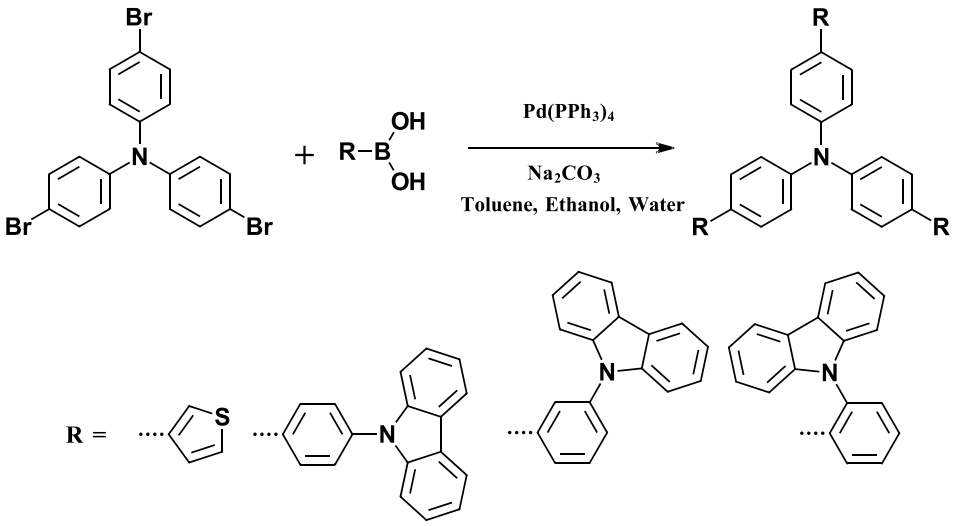

Scheme S1. Synthesis of original monomers by Suzuki reaction.

Tris(4-(thiophen-3-yl)phenyl)amine (N-Ph-3-Th).

Yield: 23%.

^{1}H NMR (400MHz, $CDCl_3$); δ (ppm): 7.50 (d, *J* = 8.6 Hz, 6H), 7.38 (m, 9H) 7.18 (d, *J* = 8.6 Hz, 76H).

^{13}C NMR (100 MHz, $CDCl_3$) δ 146.47, 141.82, 130.56, 127.28, 126.17, 126.13, 124.36, 119.38.

Tris(4'-(9*H*-carbazol-9-yl)-[1,1'-biphenyl]-4-yl)amine(N-Ph-p-Cb).

Yield: 13%.

^{1}H NMR (400 MHz, $CDCl_3$) δ (ppm): 8.17 (d, J = 7.5 Hz, 6H), 7.91 (d, J = 8.5 Hz, 6H), 7.80 (m, 3H), 7.71 (d, J = 8.5 Hz, 6H), 7.62 (m, 6H), 7.51 (m, 6H), 7.46 (m, 9H), 7.32 (m, 6H).

^{13}C NMR (100 MHz, $CDCl_3$) δ 146.80, 140.82, 139.52, 139.28, 137.25, 136.60, 135.00, 132.46, 128.50, 128.00, 127.48, 126.01, 123.50, 120.37, 120.00, 109.82.

Tris(3'-(9*H*-carbazol-9-yl)-[1,1'-biphenyl]-4-yl)amine (N-Ph-m-Cb).

Yield: 49%.

^{1}H NMR (400 MHz, $CDCl_3$) δ(ppm): 8.17 (d, *J* = 7.7 Hz Hz, 6H), 7.80 (m, 3H), 7.65 (m, 6H), 7.57 (d, *J* = 8.6 Hz, 6H), 7.54 (m, 3H), 7.49 (m, 6H), 7.42 (m, 6H), 7.31 (m, 6H), 7.26 (d, *J* = 8.6 Hz, 6H).

^{13}C NMR (100 MHz, $CDCl_3$) δ147.08, 142.40, 140.87, 138.23, 134.69, 130.25, 128.02, 125.95, 125.62, 125.54, 124.54, 123.39, 120.32, 120.00, 109.80.

Tris(2'-(9*H*-carbazol-9-yl)-[1,1'-biphenyl]-4-yl)amine (N-Ph-o-Cb).

Yield: 77%.

^{1}H NMR (400 MHz, $CDCl_3$*d*) δ(ppm): 7.98 (d, *J* = 7.7 Hz, 6H), 7.50 (m, 12H), 7.20 (m, 6H), 7.02 (m, 12H), 6.58 (d, *J* = 8.6 Hz, 6H), 5.95 (d, *J* = 8.6 Hz, 6H).

^{13}C NMR (100 MHz, $CDCl_3$) δ 146.14, 140.88, 140.39, 134.75, 132.62, 130.81, 129.67, 128.64, 128.26, 125.49, 123.32, 123.00, 119.92, 119.34, 110.00.

Tris(4-(thiophen-3-yl)phenyl)amine (N-Ph-3-Th).

Yield: 23%.

^{1}H NMR (400MH_Z, $CDCl_3$); δ (ppm): 7.50 (d, *J* = 8.6 H_Z, 6H), 7.38 (m, 9H) 7.18 (d, *J* = 8.6 H_Z, 76H).

^{13}C NMR (100 MHz, $CDCl_3$) δ 146.47, 141.82, 130.56, 127.28, 126.17, 126.13, 124.36, 119.38.

Computational methodology.

All the computational studies were performed with Gaussian 16 package of programs[49] using the density functional theory method (DFT). The hybrid functional B3LYP, which combines Becke's three-parameter hybrid exchange functional[4949] and Lee–Yang–Paar's gradient-corrected correlation functional,[49] and 6-31G split valence basis set supplemented by d-polarization functions were used for geometry optimizations of isolated molecules in a gas phase. No constraints were used, and all structures were free to optimize. The force constants and vibrational frequency analysis for stationary points have been calculated after optimizations to check that they are true energy minima.

Electronic structure for the optimized geometries were calculated at the same level of theory. The restricted Hartree-Fock formalism was used for the neutral states of the molecules, and unrestricted Hartree-Fock formalism was used for radical cation calculations.

Visualization of the orbital coefficients and spin density distribution (in radical cations) were performed with GaussView 6.0 software.

Soft-template electropolymerization.

Two solvents were investigated: dichloromethane (CH_2Cl_2) and dichloromethane saturated with water (CH_2Cl_2 + H_2O sat.). Because the solubility of water in dichloromethane is ultra-low, the later was very easily prepared by mixing water and dichloromethane, and after decantation the aqueous phase was discarded. Tetrabutylammonium perchlorate (Bu_4NClO_4) (0.1 M) as the supporting electrolyte and monomer (0.005 M) were added to the solvent. Three electrodes were connected to an Autolab potentiostat-galvanostat model PGSTAT100 (Metrohm). 2 cm^2 gold-coated silicon wafer

as the working electrode, glassy carbon rod as the counter-electrode, and saturated calomel electrode (SCE) as the reference electrode. First, the oxidation potential for each monomer were determined by cyclic voltammetry. Then, two electrodeposition methods were investigated (by cyclic voltammetry and at constant potential). The experiments by cyclic voltammetry were performed from –1 V to E^{ox}, at a scan rate of 20 mV s^{-1} with different numbers of scans (1, 3 and 5). The experiments at constant potential were performed with a potential $E = E^{ox}$, and with different deposition charges (12.5, 25, 50, 100, 200 and 400 mC cm^{-2}). Then, the substrates were abundantly washed with CH_2Cl_2.

Smooth surfaces with each monomer were prepared using a two-step process. First deposition at constant potential with a low deposition charge of 1 mC cm^{-2}. Then, in order to have polymers in the same state (i.e. dedoped state) as in cyclic voltammetry experiments, the deposits were reduced with one back scan from E^{ox} to –1 V in a solution free of monomer.

Surface characterization.

Samples were observed by transmission electron microscopy (TEM) prior to electrodeposition using a JEOL JSM-1400 TEM. For imaging, a drop of 0.45 µm-filtered solution was deposited onto a 400 mesh TEM copper grid with a carbon support film and the exceeding liquid was absorbed with a paper filter to avoid excessive salt deposition onto the TEM grids.

The surface structures were imaged with a JEOL JSM-6700F scanning electron microscope (SEM). The surface wettability was characterized by measuring apparent contact angles (θ) using a KRÜSS DSA30 goniometer. Three probes of liquids of different surface tensions (γ_{LV}) were used: water (72.8 mN/m), diiodomethane (50.0 mN/m) and *n*-hexadecane (27.6 mN/m).

Each value is given here is a mean value of five measurements. For characterizing the water adhesion, a water droplet was placed on the substrate and the substrate was inclined until the droplet moved. If the droplet moved, that indicated extremely high water adhesion (parahydrophobic or sticky superhydrophobic). For smooth surfaces, the apparent contact angles are called Young' angles (θ^Y). Their surface energy γ_{SV} were calculated with the Owens-Wendt equation as well as their polar ($\gamma_{SV,P}$) and dispersive ($\gamma_{SV,D}$) parts.

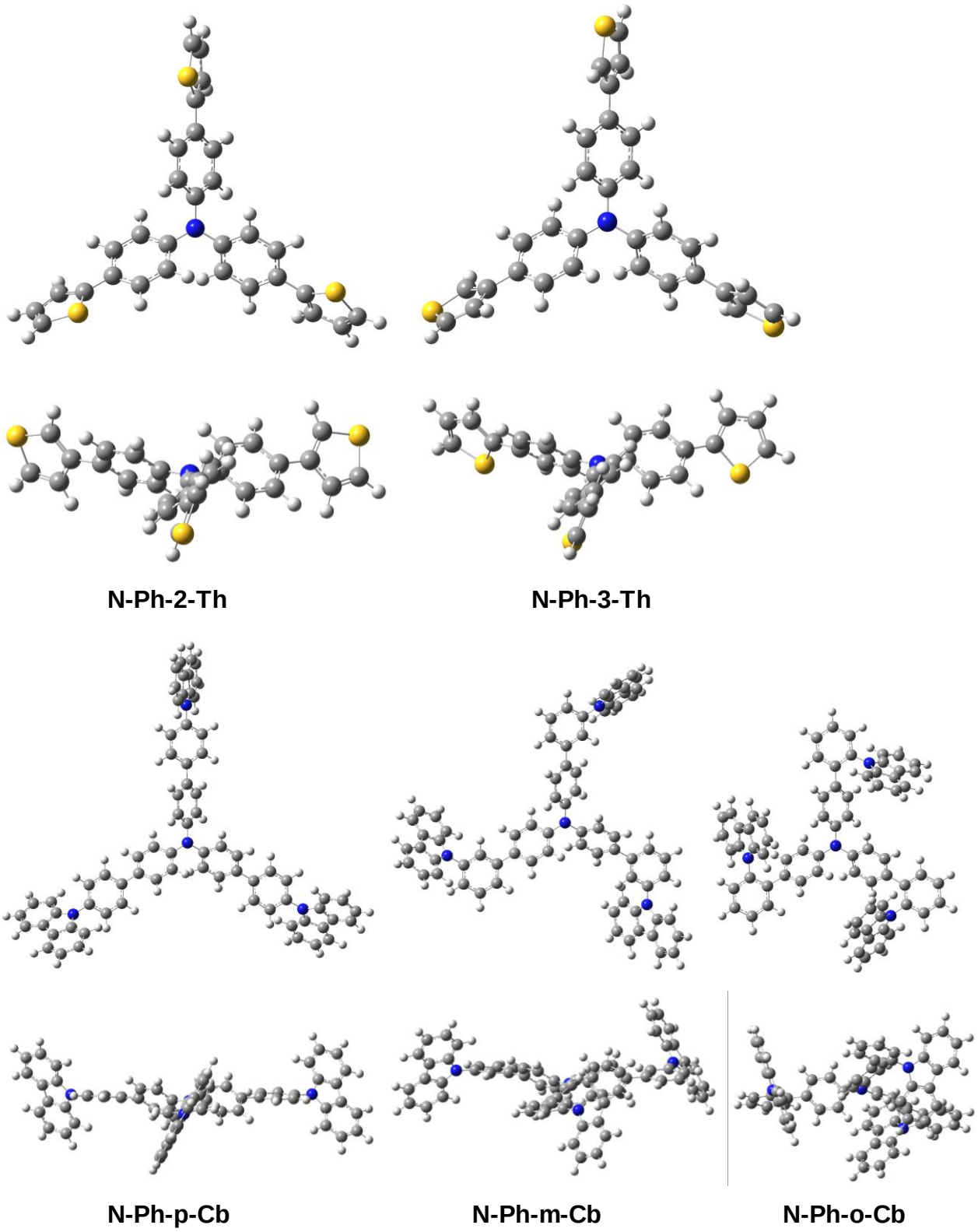

Figure S1. B3LYP/6-31G(d) optimized geometries of studied monomers in a gas phase. For clarity, two views of each structure are shown, i.e. perpendicular to the triphenylamine plane and in the plane.

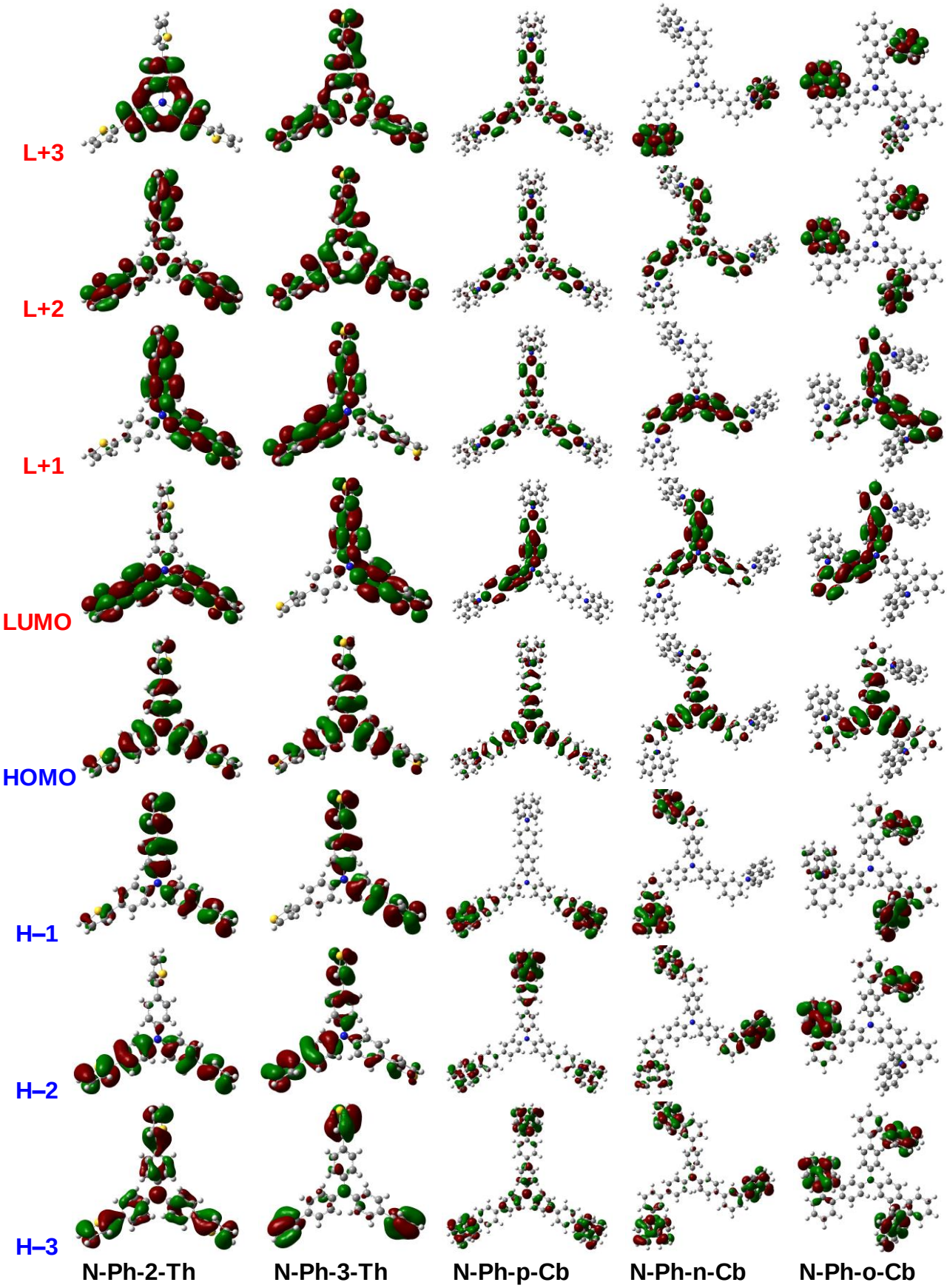

Figure S2. Orbital coefficients distribution in studied monomers, from HOMO–3 to LUMO+3 orbitals, calculated at B3LYP/6-31G(d) level in a gas phase.

Electrochemical characterization

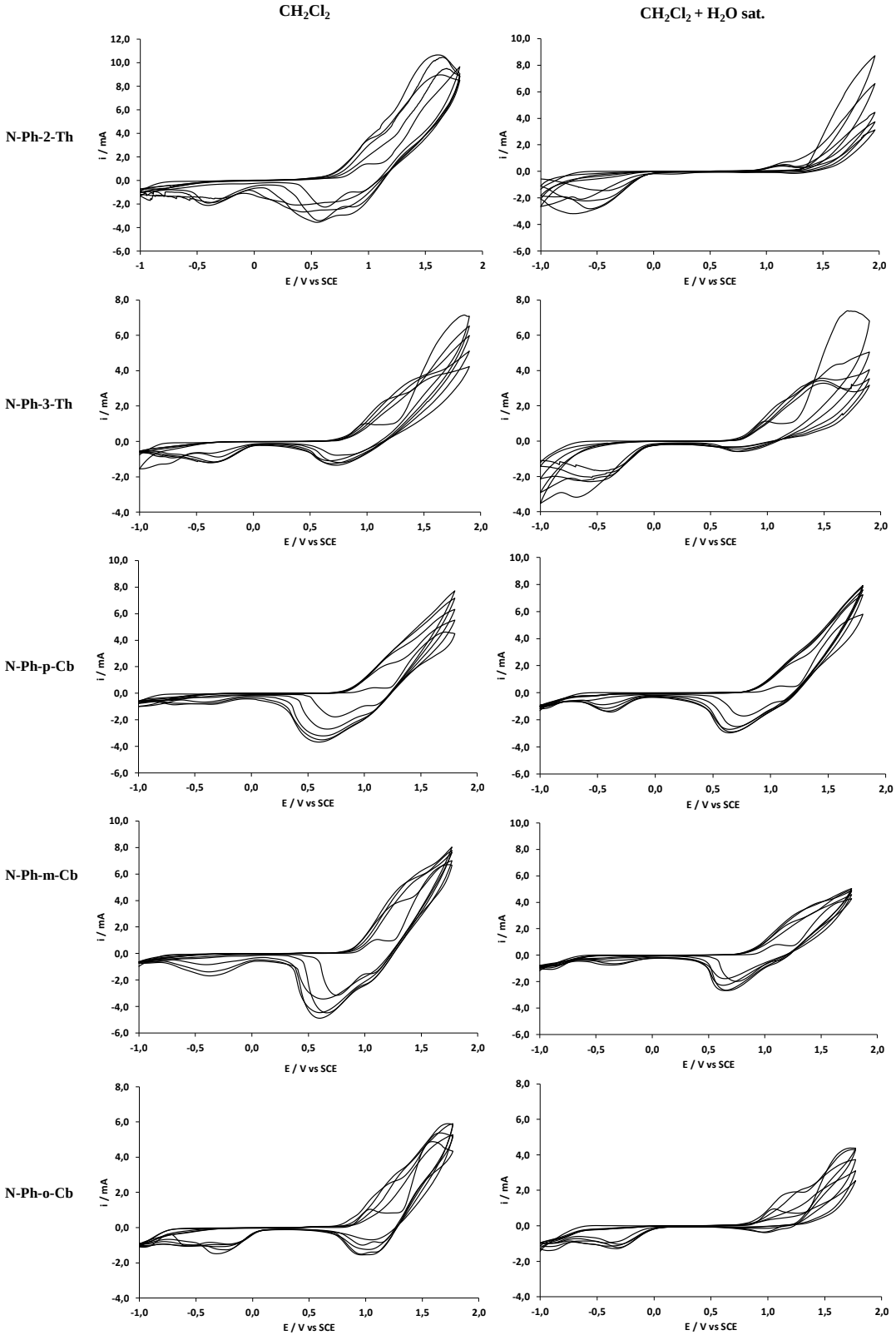

Figure S3. Cyclic voltammograms of studied compounds on cycling. Electrodepositions were performed in CH_2Cl_2 or (CH_2Cl_2 + H_2O sat.) as solvents and with 0.1 M of Bu_4NClO_4 as an

electrolyte. The range of potential scancs was from –1 V to E^{ox}, scan rate 20 mV s^{-1}. First five scans are shown.

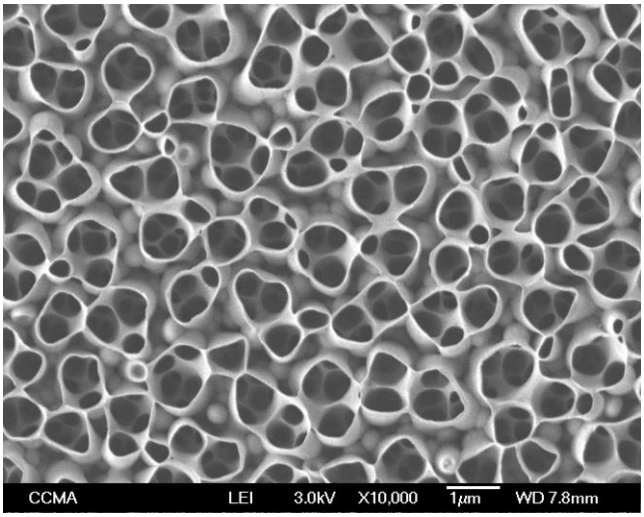

1 scan

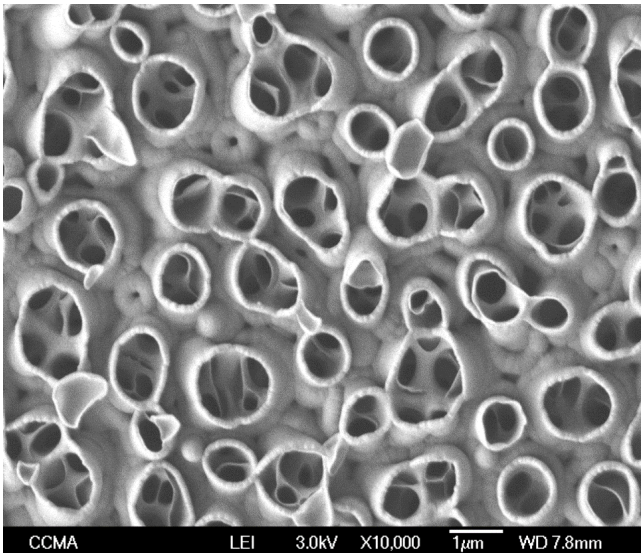

3 scans

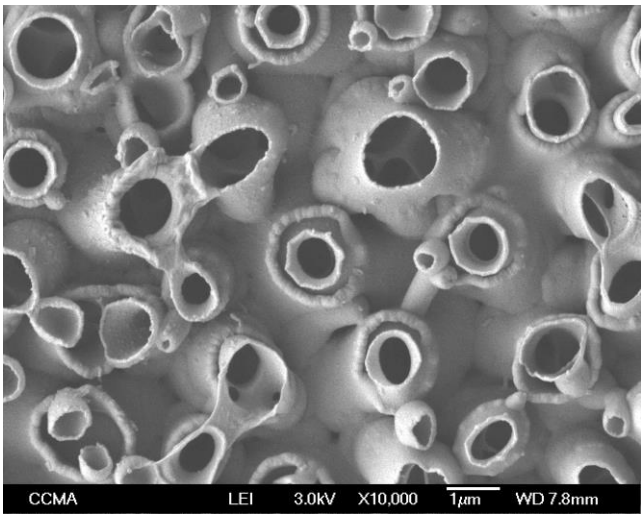

5 scans

Figure S4. SEM images of electrodeposited surfaces from **N-Ph-3-Th** by CV in (CH_2Cl_2 + H_2O sat.) with 0.1 M of Bu_4NClO_4 for 1, 3 and 5 scans in the potential range from –1 V to E^{ox} at the scan rate of 20 mV s^{-1}. Magnification is ×10,000.

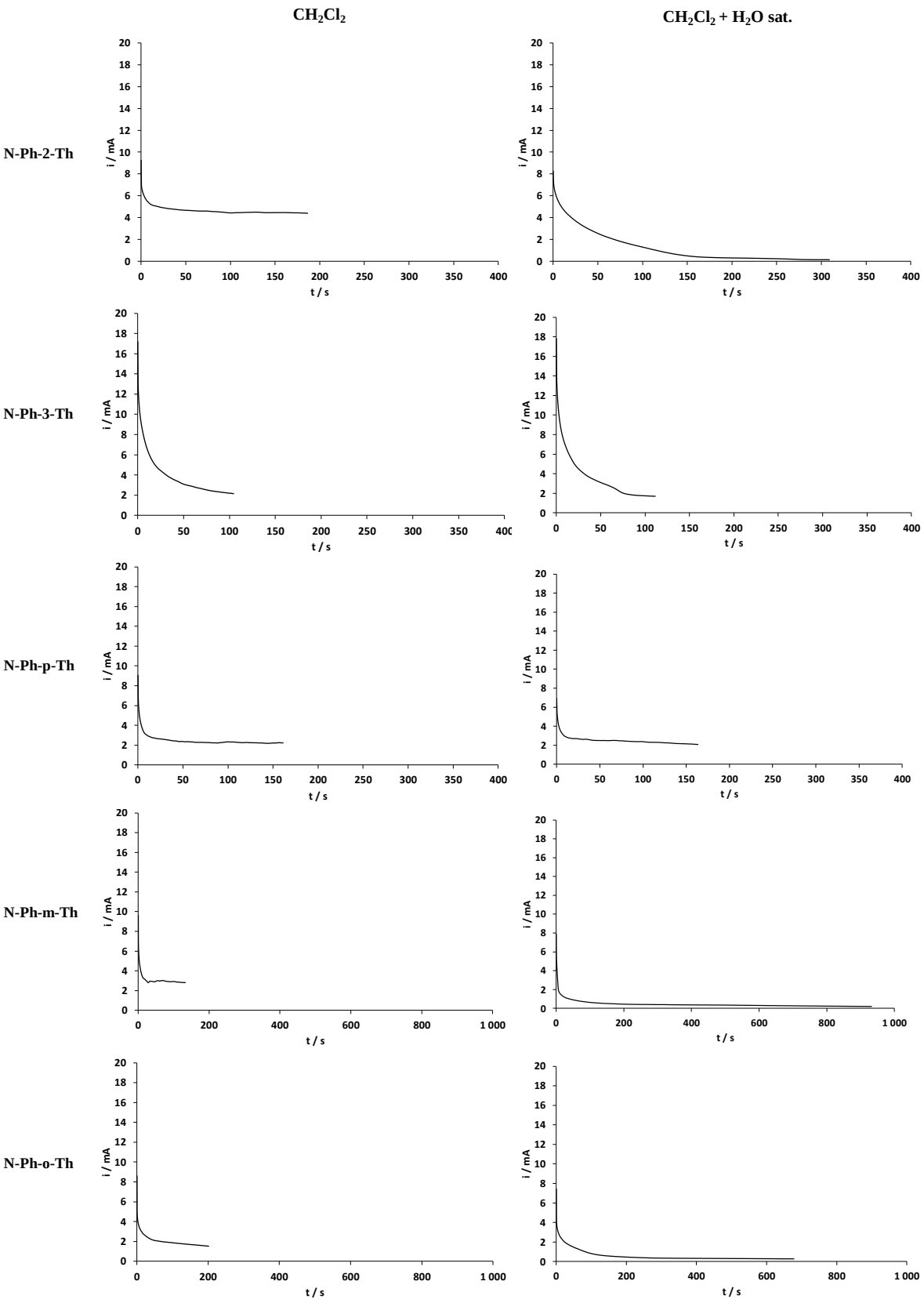

Figure S5. Potentiostatic electrodeposition of studied monomers at applied potentials E^{ox} (currents *vs* time curves at constant potential E^{ox} are shown) in CH_2Cl_2 or (CH_2Cl_2 + H_2O sat.) as solvents, with 0.1 M of Bu_4NClO_4 as an electrolyte.

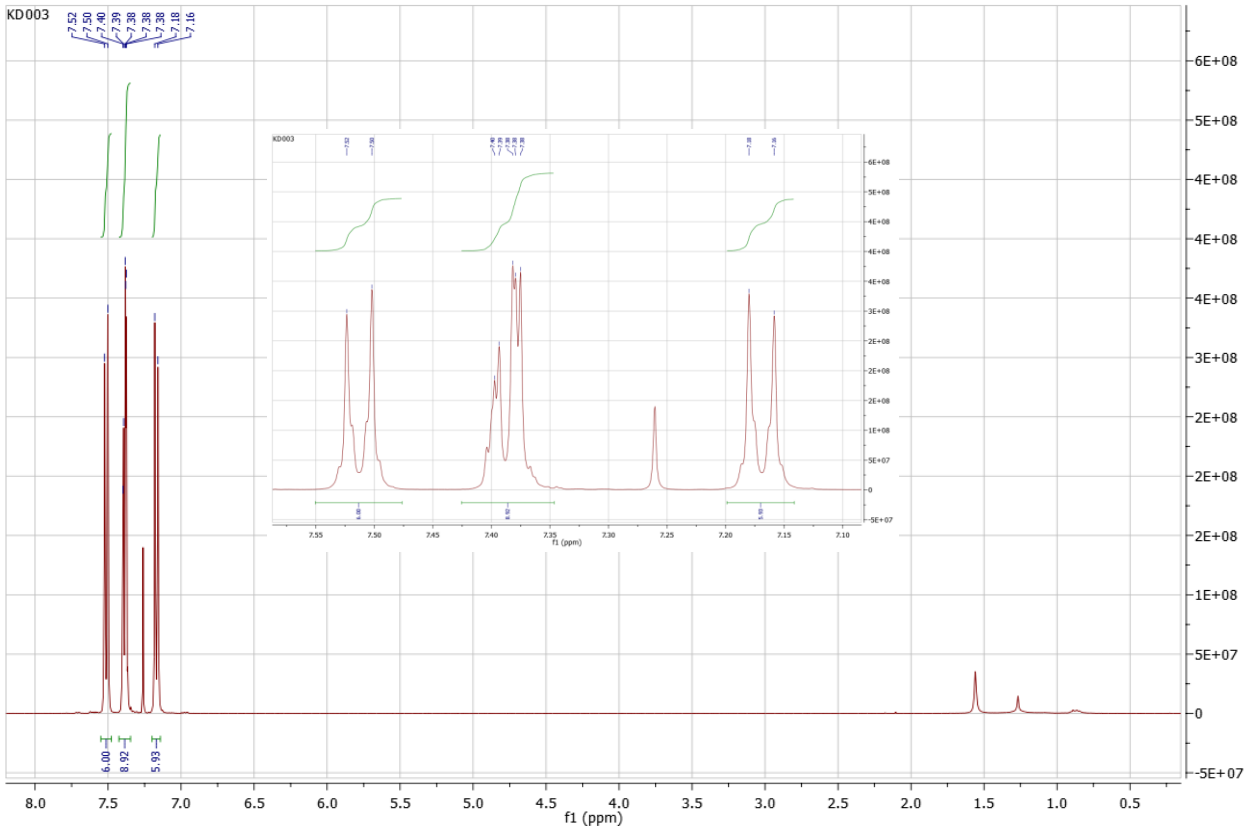

Figure S6. ^{1}H NMR spectrum of **N-Ph-3-Th** in $CDCl_3$.

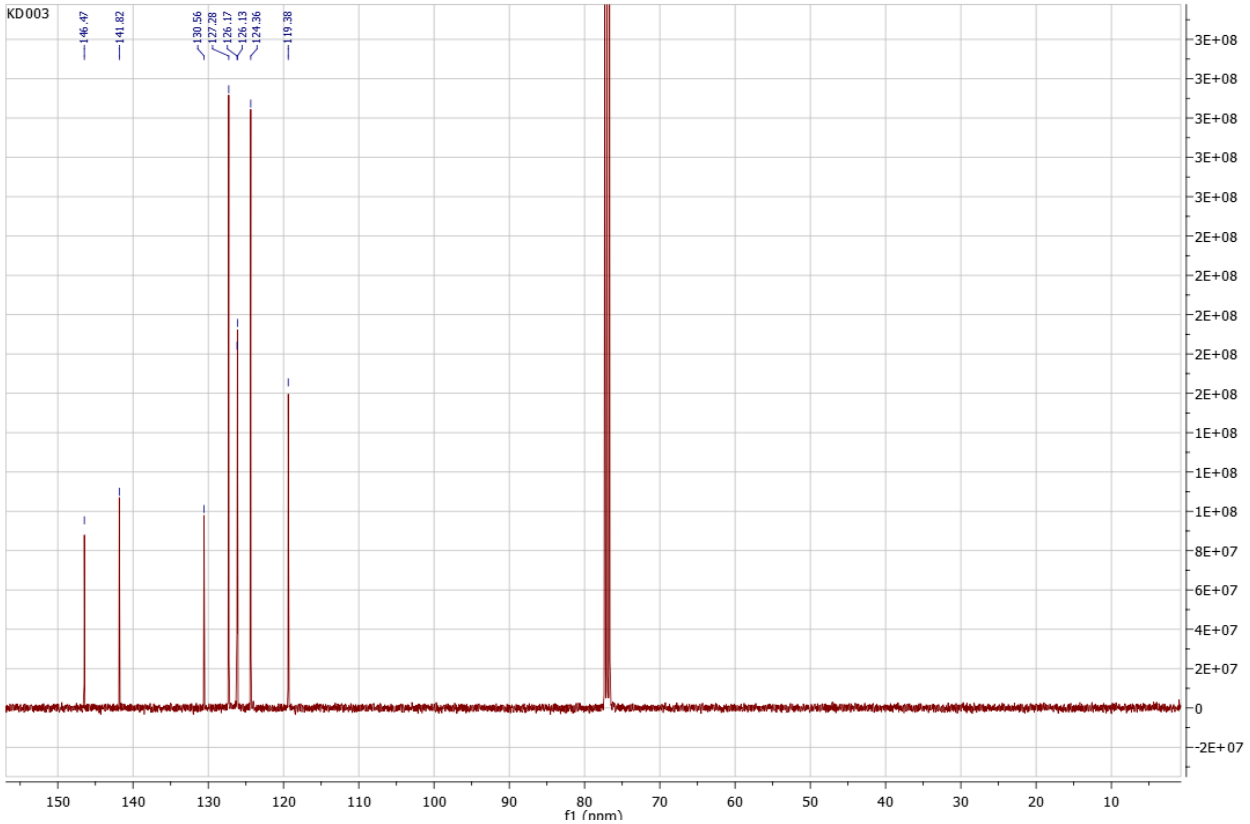

Figure S7. ^{13}C NMR spectrum of **N-Ph-3-Th** in $CDCl_3$.

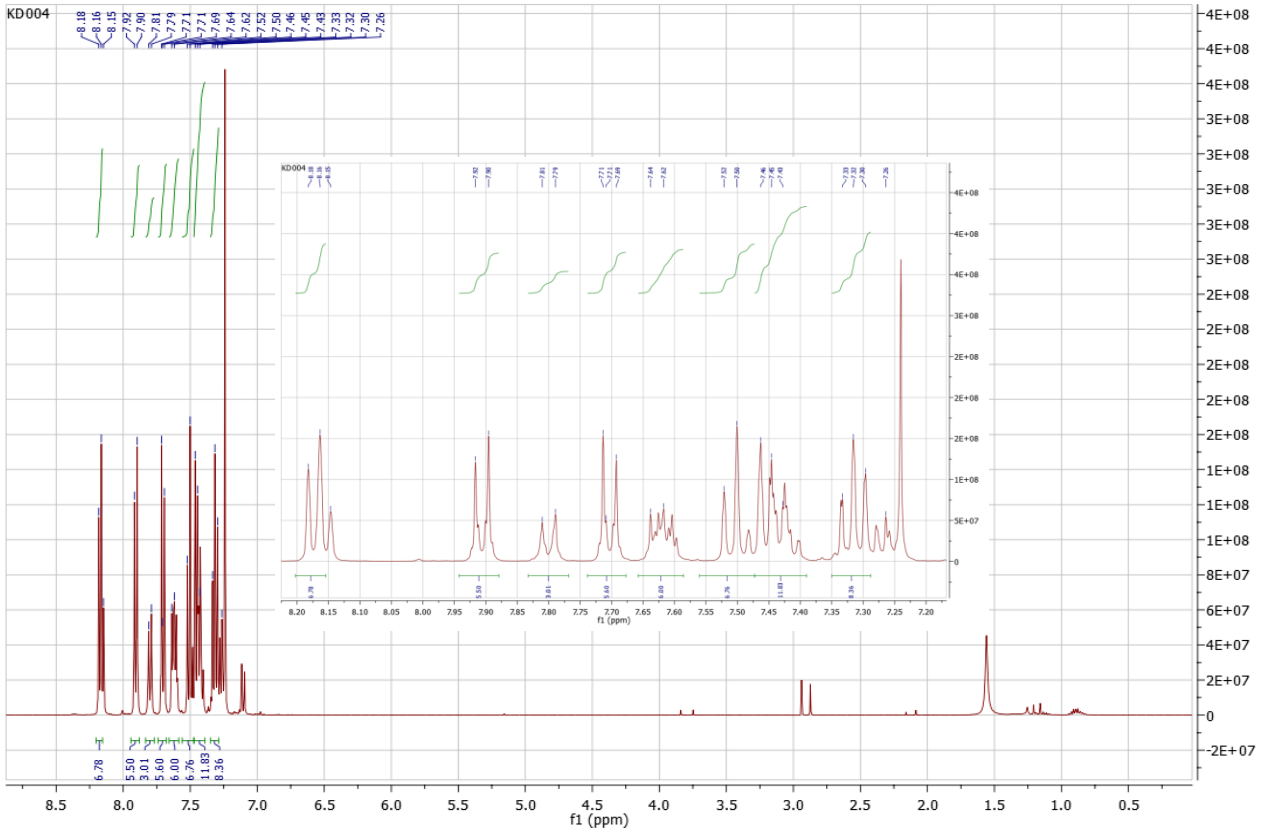

Figure S8. ^{1}H NMR spectrum of **N-Ph-p-Cb** in $CDCl_3$.

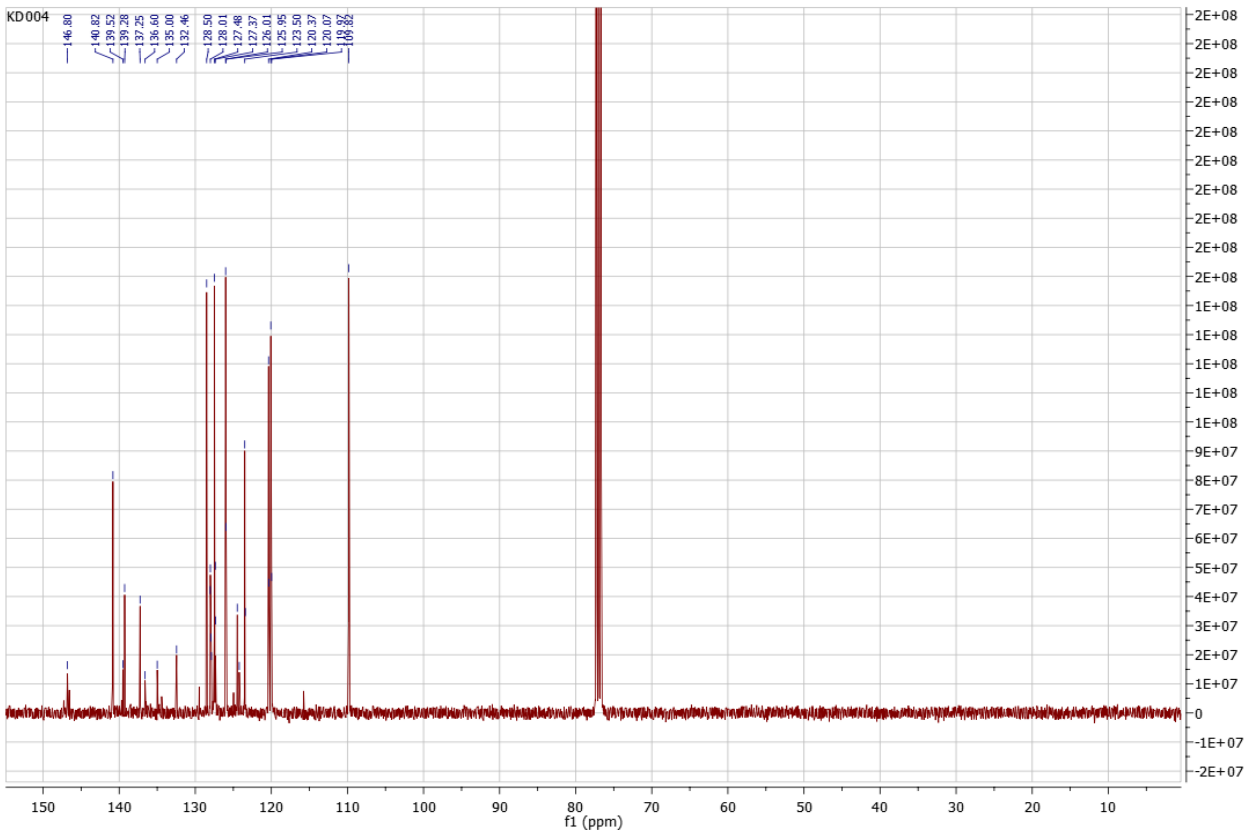

Figure S9. ^{13}C NMR spectrum of **N-Ph-p-Cb** in $CDCl_3$.

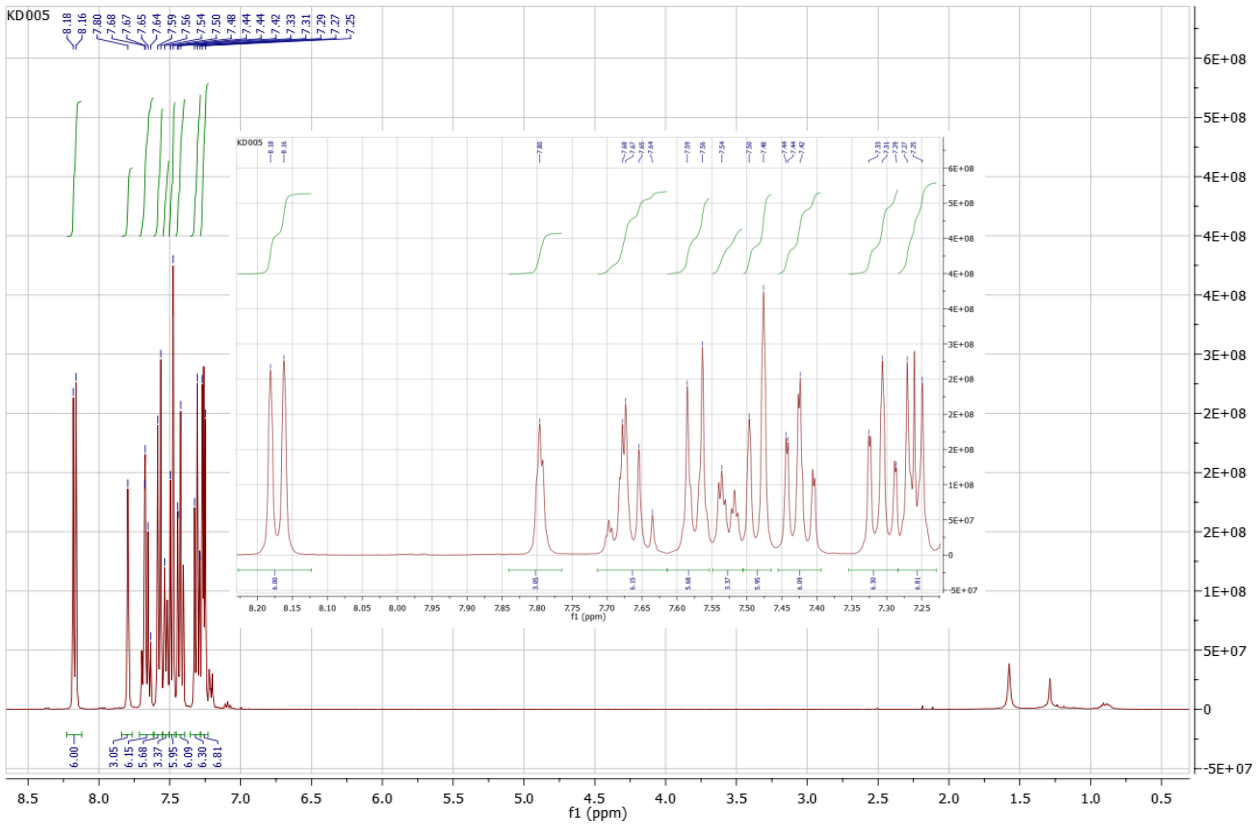

Figure S10. ^{1}H NMR spectrum of **N-Ph-m-Cb** in $CDCl_3$.

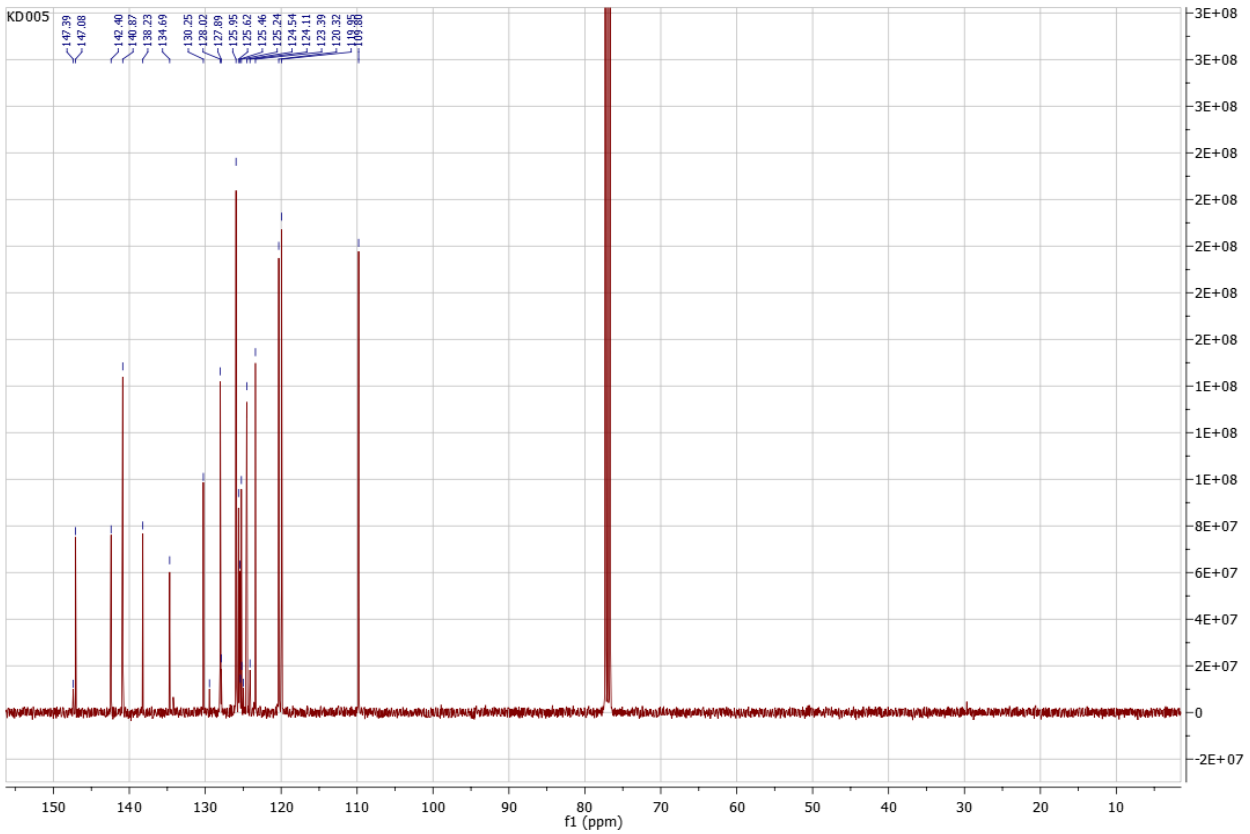

Figure S11. ^{13}C NMR spectrum of **N-Ph-m-Cb** in $CDCl_3$.

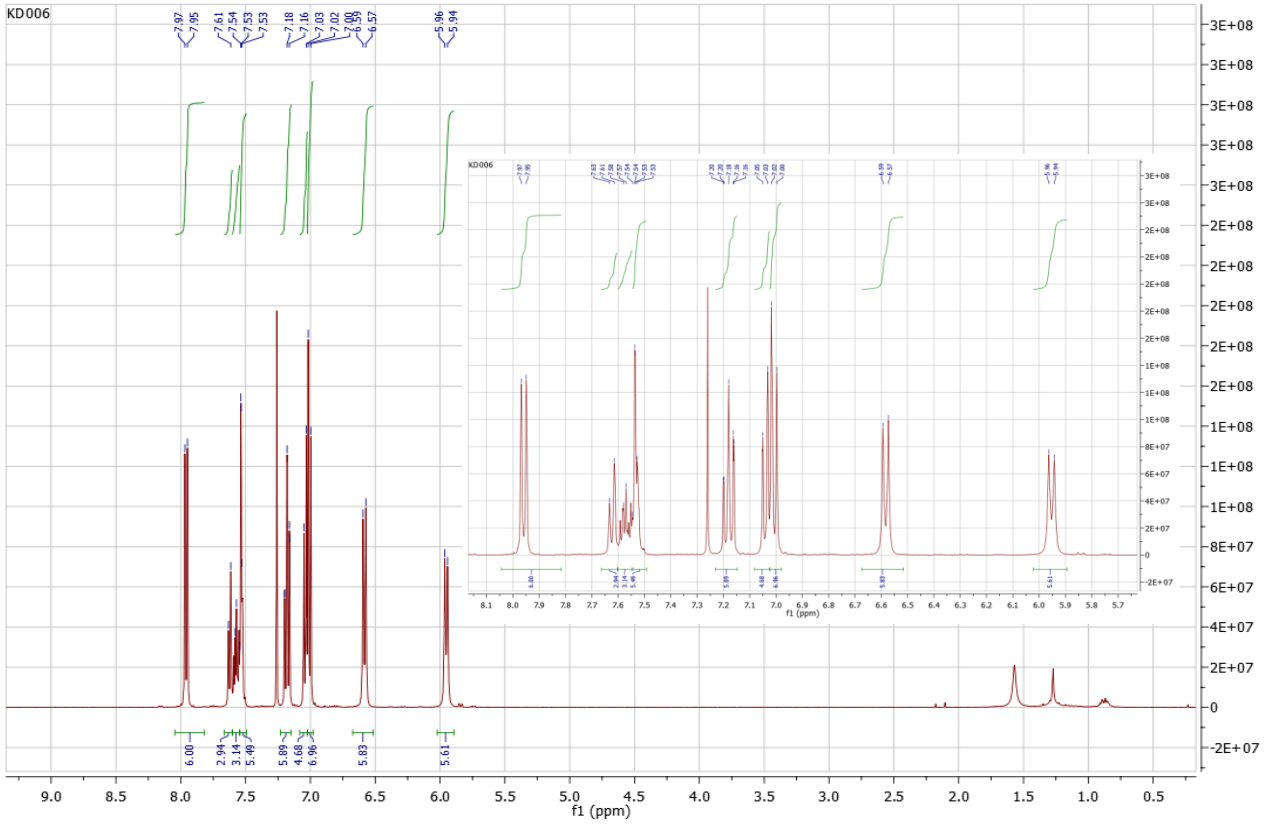

Figure S12. ^{1}H NMR spectrum of **N-Ph-o-Cb** in $CDCl_3$.

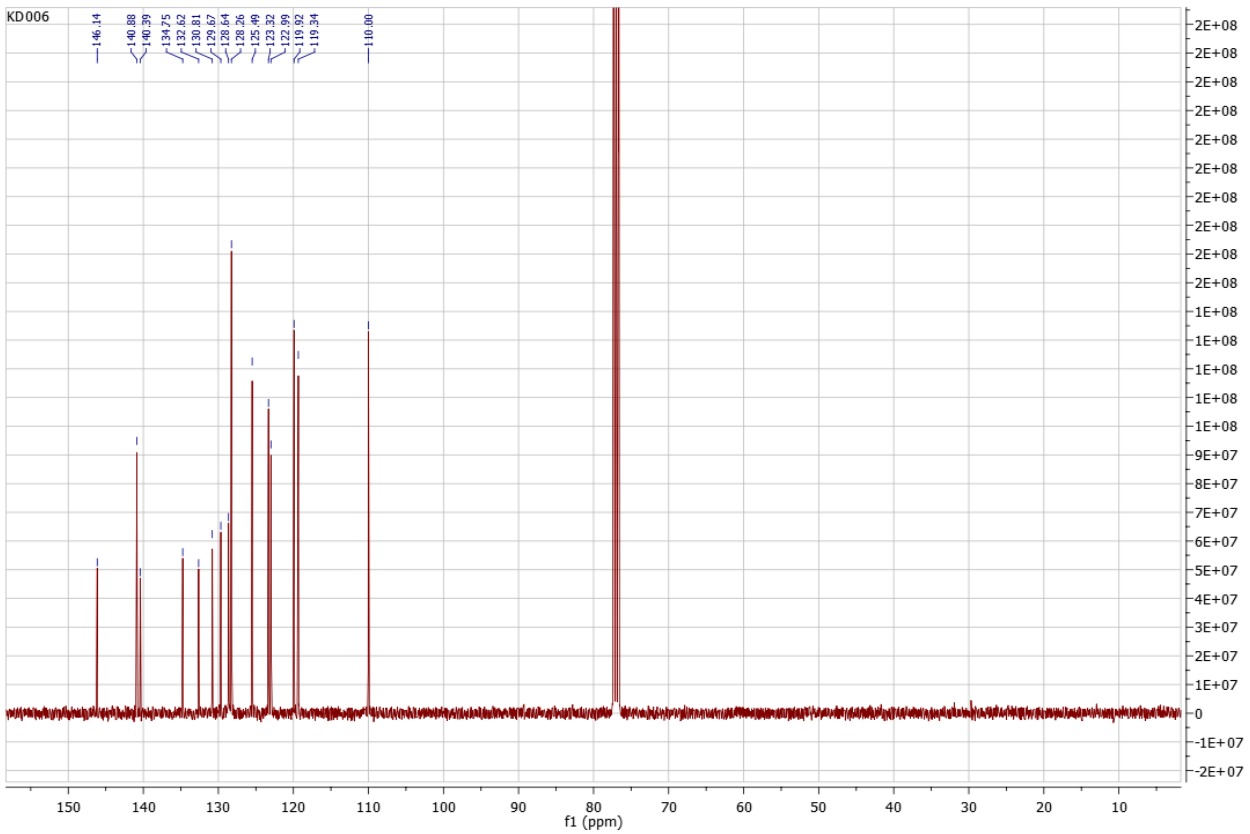

Figure S13. ^{1}H NMR spectrum of **N-Ph-o-Cb** in $CDCl_3$.

N-Ph-2-Th, neutral state

E_{total} = −2405.1372798 Hartree // B3LYP/6-31G(d)

C	1.41497900	-0.12292300	0.14377400
N	0.00032700	-0.00013300	0.14659600
C	-0.60070000	1.28641800	0.14391700
C	-0.81348000	-1.16378600	0.14388000
C	-1.73092900	1.55370200	0.93437100
C	-2.32506800	2.80925900	0.91876300
C	-1.80261700	3.85995300	0.14117500
C	-0.66527400	3.58302100	-0.63884100
C	-0.08185500	2.32165300	-0.65016600
C	-1.97002400	-1.23141000	-0.64942800
C	-2.77098000	-2.36713900	-0.63803000
C	-2.44189900	-3.49102200	0.14125200
C	-1.27020500	-3.41876800	0.91807600
C	-0.47962400	-2.27666200	0.93365200
C	2.05192000	-1.09112300	-0.64896200
C	3.43600600	-1.21651600	-0.63780100
C	4.24472300	-0.36887400	0.14074900
C	3.59621000	0.61011700	0.91697500
C	2.21181100	0.72342900	0.93274500
C	-2.42935500	5.18565500	0.15997600
C	-3.27691500	-4.69643100	0.16006100
C	5.70617900	-0.48894400	0.15950300
C	-3.18344000	5.76561300	1.15589100
C	-3.64480100	7.07590300	0.83919200
C	-3.24256100	7.49574700	-0.39848100
S	-2.29594400	6.28534400	-1.20312200
C	-3.40183100	-5.63989700	1.15560900
C	-4.30631200	-6.69423100	0.83890700
C	-4.87163000	-6.55511900	-0.39840900
S	-4.29680600	-5.12988800	-1.20270800
C	6.58564300	-0.12411100	1.15463600

C	7.95101800	-0.38021300	0.83816000
C	8.11331100	-0.94062100	-0.39856800
S	6.59163800	-1.15666600	-1.20259600
H	-2.14950800	0.76597100	1.55249500
H	-3.21533100	2.97833800	1.51713400
H	-0.22549300	4.36937700	-1.24633000
H	0.78850400	2.13509400	-1.27090400
H	-2.24389000	-0.38400300	-1.26954300
H	-3.67233500	-2.37889700	-1.24484500
H	-0.97135800	-4.27458400	1.51597700
H	0.41222800	-2.24579500	1.55127400
H	1.45505400	-1.75256100	-1.26854800
H	3.89694600	-1.99151100	-1.24420400
H	4.18791200	1.29742400	1.51422500
H	1.73916000	1.48074500	1.54988900
H	-3.37815400	5.27709400	2.10452400
H	-4.24321500	7.68239900	1.51066200
H	-3.44453700	8.43876900	-0.88833500
H	-2.88090500	-5.56483900	2.10401400
H	-4.53218600	-7.51596800	1.51012900
H	-5.58775600	-7.20114500	-0.88815600
H	6.26007300	0.29041600	2.10260400
H	8.77556400	-0.16403800	1.50913200
H	9.03091200	-1.23807200	-0.88803000

N-Ph-3-Th, neutral state

E_{total} = -2405.1346219 Hartree // B3LYP/6-31G(d)

C	1.04840400	-0.95887100	-0.01410000
N	-0.00272300	-0.00384200	0.01441600
C	0.29836800	1.38430200	0.03065400
C	-1.35540100	-0.43726800	0.03069200
C	-0.42265800	2.26714400	0.85019500
C	-0.13023500	3.62682000	0.85490200
C	0.90131100	4.15982300	0.06309300
C	1.62633100	3.26368300	-0.74138200
C	1.32676800	1.90658500	-0.77077900
C	-2.33080100	0.22126500	-0.73587300
C	-3.65566800	-0.19845500	-0.70641200
C	-4.06050200	-1.30302300	0.06294700
C	-3.07439900	-1.95845100	0.82001700
C	-1.75056700	-1.53221100	0.81550600
C	0.95776100	-2.10402500	-0.82124700
C	1.98542500	-3.04091800	-0.83824600
C	3.15070000	-2.86820100	-0.07174400
C	3.23665500	-1.71003300	0.72010800
C	2.20514400	-0.77911500	0.76199400
C	1.20451200	5.60474800	0.07538600
C	-5.46345900	-1.76290000	0.07456300
C	4.23636000	-3.86850900	-0.09664100
C	1.00340900	6.46513200	1.21190300
C	1.35682200	7.76240000	0.98182700
S	1.94590400	7.98430000	-0.63566000
C	1.71243500	6.30638400	-0.99423100
C	-6.09525000	-2.40830000	1.19558100
C	-7.39815700	-2.74211100	0.96810600
S	-7.90321800	-2.28402300	-0.62801200
C	-6.33723400	-1.63475800	-0.98112100
C	4.54922500	-4.69655400	-1.23190500
C	5.59479100	-5.54534100	-1.01489600
S	6.23594400	-5.36855000	0.58828500
C	5.07888100	-4.13463800	0.95868000
H	-1.21981100	1.88280200	1.47846100
H	-0.72192100	4.28797400	1.48179800
H	2.44641600	3.63499200	-1.34965200
H	1.89840300	1.23979300	-1.40837600
H	-2.04613600	1.07244600	-1.34607700
H	-4.39398200	0.34805400	-1.28659800
H	-3.34435300	-2.82368500	1.41893400

H	-1.01222400	-2.05316700	1.41661100
H	0.07295400	-2.26018700	-1.43001700
H	1.87514900	-3.92862800	-1.45471000
H	4.13218200	-1.53015900	1.30838600
H	2.29625800	0.10167900	1.38951400
H	0.63749300	6.11281600	2.17005000
H	1.32297900	8.59742300	1.66850300
H	1.92719300	5.93499200	-1.98693500
H	-5.59628300	-2.58398700	2.14227700
H	-8.09669000	-3.21363600	1.64607800
H	-6.13418900	-1.22710000	-1.96199100
H	4.02739600	-4.63131000	-2.18032400
H	6.03817800	-6.25134800	-1.70402000
H	5.05813700	-3.69811800	1.94789200

N-Ph-p-Cb, neutral state

E_{total} = −2991.6888124 Hartree // B3LYP/6-31G(d)

C	1.23474800	-0.70156900	-0.00262200
N	0.00009600	-0.00047300	-0.00314600
C	-0.01005500	1.41933900	-0.00280800
C	-1.22442900	-0.71914100	-0.00273600
C	-0.92383600	2.13124900	0.79100500
C	-0.93436700	3.52145900	0.78185000
C	-0.03029900	4.25940700	-0.00215900
C	0.88420000	3.53478600	-0.78652100
C	0.89348200	2.14456400	-0.79630800
C	-2.30439300	-0.29899400	-0.79593100
C	-3.50382800	-1.00194700	-0.78591500
C	-3.67407800	-2.15638100	-0.00174000
C	-2.58279200	-2.57068700	0.78185400
C	-1.38400900	-1.86660600	0.79085800
C	2.30823000	-0.26573600	0.79085700
C	3.51749800	-0.95165400	0.78183900
C	3.70443100	-2.10400000	-0.00158300
C	2.61955200	-2.53410700	-0.78557500
C	1.41095800	-1.84702800	-0.79560800
C	-4.95194400	-2.90602000	-0.00113900
C	-0.04078000	5.74088000	-0.00167800
C	4.99273900	-2.83554700	-0.00102800
C	-6.18623900	-2.24213300	-0.11445700
C	-7.38942900	-2.94137800	-0.10674700
C	-7.39299900	-4.33794700	0.00002000
C	-6.17216600	-5.01626200	0.10618700
C	-4.97468800	-4.30727700	0.11276900
C	1.15116700	6.47801900	-0.11527100
C	1.14700700	7.86962900	-0.10741700
C	-0.06073000	8.57086100	-0.00031100
C	-1.25847100	7.85257800	0.10607400
C	-1.24301600	6.46103900	0.11254700
C	5.03523700	-4.23647000	-0.11341200
C	6.24257600	-4.92851700	-0.10574200
C	7.45370300	-4.23295100	0.00000000
C	7.43042400	-2.83645500	0.10527000
C	6.21750700	-2.15421500	0.11193600
N	-8.61701800	-5.05597500	0.00062200
N	-0.07072000	9.98990400	0.00045000
N	8.68773500	-4.93363500	0.00056000
C	-9.03489700	-5.96304300	0.98244500
C	-10.31089400	-6.47059300	0.62794700
C	-10.67911300	-5.84395000	-0.62447200
C	-9.61351600	-4.97834000	-0.98036400
C	-0.64758600	10.80514300	0.98228000
C	-0.44937000	12.16402400	0.62791300
C	0.27756900	12.16984400	-0.62442400
C	0.49470700	10.81427400	-0.98041500
C	9.68272400	-4.84076300	0.98175100
C	10.76034100	-5.69203400	0.62747700
C	10.40127700	-6.32552400	-0.62416200

C	9.11847800	-5.83624600	-0.97980700
C	-8.39949500	-6.34439700	2.16753100
C	-9.05316100	-7.26153200	2.98787500
C	-10.31135100	-7.78556000	2.64467000
C	-10.94529100	-7.39137900	1.47000200
C	-11.79314400	-5.94853500	-1.46551300
C	-11.82865200	-5.20353500	-2.64059400
C	-10.75735100	-4.36151200	-2.98520100
C	-9.63713700	-4.23830200	-2.16586300
C	11.04869000	-7.23861300	-1.46468300
C	10.42069500	-7.64321200	-2.63900800
C	9.15547500	-7.13717400	-2.98338300
C	8.48885000	-6.22805000	-2.16455900
C	9.69565100	-4.09874000	2.16613800
C	10.81718100	-4.20519700	2.98602200
C	11.90019200	-5.03278100	2.64301600
C	11.87543500	-5.77993400	1.46902600
C	-1.29555200	10.44534200	2.16729200
C	-1.76319800	11.46984700	2.98770200
C	-1.58817800	12.82155000	2.64461200
C	-0.92984600	13.17367500	1.47000100
C	0.74388200	13.18710200	-1.46530800
C	1.40705800	12.84559800	-2.64033000
C	1.60092100	11.49688200	-2.98504300
C	1.14760900	10.46496700	-2.16587700
H	-1.61771900	1.58830800	1.42470100
H	-1.63200100	4.04468400	1.42980000
H	1.57433000	4.06821400	-1.43420800
H	1.59503300	1.61183400	-1.43024200
H	-2.19385800	0.57504400	-1.42971200
H	-4.31094700	-0.67072700	-1.43333200
H	-2.68702700	-3.43658800	1.42967400
H	-0.56673600	-2.19628300	1.42427700
H	2.18497200	0.60695200	1.42414300
H	4.31954600	-0.60871100	1.42946600
H	2.73638800	-3.39880500	-1.43285000
H	0.59876100	-2.18847500	-1.42932400
H	-6.20732900	-1.15750200	-0.16840600
H	-8.33316100	-2.40763400	-0.16061900
H	-6.16676300	-6.10043700	0.16048000
H	-4.03819700	-4.85491900	0.16628400
H	2.10108400	5.95408000	-0.16953600
H	2.08103300	8.42015400	-0.16143800
H	-2.20016400	8.38985400	0.16061700
H	-2.18545400	5.92370700	0.16626700
H	4.10656800	-4.79729600	-0.16662200
H	6.25244300	-6.01271800	-0.15882400
H	8.36653100	-2.28941500	0.15876700
H	6.22326000	-1.06933800	0.16477100
H	-7.43304400	-5.93686500	2.44500700
H	-8.57817600	-7.57404900	3.91395800
H	-10.79330700	-8.50057300	3.30532600
H	-11.92299200	-7.78933600	1.21076200
H	-12.61753900	-6.60738000	-1.20519400
H	-12.68851100	-5.27547300	-3.30048900
H	-10.79898200	-3.79494600	-3.91158000
H	-8.80989200	-3.59394900	-2.44438500
H	12.03172500	-7.62258500	-1.20453400
H	10.91276700	-8.35239600	-3.29848800
H	8.68520100	-7.45755000	-3.90918400
H	7.51693900	-5.83435700	-2.44293700
H	8.85943800	-3.46553200	2.44343200
H	10.85060800	-3.63674800	3.91157900
H	12.76073700	-5.09180200	3.30329400
H	12.70897500	-6.42766100	1.20993200
H	-1.42568600	9.40456100	2.44467200
H	-2.27133100	11.21457400	3.91374000
H	-1.96659100	13.59631900	3.30531600
H	-0.78578300	14.21940600	1.21084000
H	0.58527200	14.23041100	-1.20488900

H	1.77462800	13.62635900	-3.30009800
H	2.11257100	11.24984600	-3.91137700
H	1.29224800	9.42644600	-2.44453300

N-Ph-m-Cb, neutral state

E_{total} = −2991.688235 Hartree // B3LYP/6-31G(d)

C	-0.10834200	1.41542500	-0.16114100
N	0.00071200	-0.00024600	-0.15937400
C	1.28125700	-0.61357900	-0.16034500
C	-1.17081900	-0.80238400	-0.16034000
C	1.53539600	-1.74493200	-0.95232500
C	2.78908800	-2.34584200	-0.94359800
C	3.84233100	-1.83892600	-0.16290900
C	3.57766900	-0.70104700	0.61864300
C	2.32308700	-0.10210400	0.63009800
C	-1.24898600	-1.96051500	0.62992700
C	-2.39544200	-2.74690700	0.61894200
C	-3.51340500	-2.40639600	-0.16190700
C	-3.42545100	-1.24093800	-0.94277900
C	-2.27782600	-0.45625600	-0.95192100
C	0.74399200	2.20095400	-0.95384100
C	0.63778200	3.58715500	-0.94542100
C	-0.32724200	4.24612700	-0.16427700
C	-1.17990300	3.44827800	0.61804700
C	-1.07161400	2.06228300	0.62973000
C	-4.73737700	-3.24383700	-0.16332300
C	5.17987600	-2.47958300	-0.16476300
C	-0.44140600	5.72476700	-0.16650100
C	-4.64884900	-4.64182600	-0.06687100
C	-5.79796000	-5.43849800	-0.06236300
C	-7.06182500	-4.84619500	-0.17108600
C	-7.15804600	-3.46008600	-0.28779000
C	-6.01364900	-2.66510500	-0.27671200
C	6.34615900	-1.70370200	-0.06791400
C	7.61080800	-2.30021400	-0.06322900
C	7.73019400	-3.69081400	-0.17252500
C	6.57811600	-4.46737300	-0.29007700
C	5.31727500	-3.87408300	-0.27914700
C	-1.69666600	6.34637400	-0.06873000
C	-1.81297700	7.73977300	-0.06431500
C	-0.66872700	8.53893700	-0.17416400
C	0.57998100	7.92995300	-0.29254300
C	0.69716900	6.54143200	-0.28170100
N	-5.67838900	-6.85123500	0.04005400
N	-3.09660800	8.34159000	0.03953300
N	8.77430900	-1.49010700	0.03988700
C	-6.18438600	-7.78455200	-0.87240600
C	-5.85410600	-9.09013300	-0.42721900
C	-5.11817900	-8.93787500	0.81052600
C	-5.02819100	-7.54564400	1.06667000
C	9.83566000	-1.46081800	-0.87243500
C	10.80125400	-0.52257600	-0.42618000
C	10.30120400	0.03767700	0.81190500
C	9.05044200	-0.58069600	1.06733300
C	-3.65377700	9.24585800	-0.87236200
C	-4.94920100	9.61187700	-0.42538700
C	-5.18314200	8.89843600	0.81279200
C	-4.02151000	8.12525600	1.06744000
C	-4.54841000	-9.84319100	1.71350100
C	-3.90995300	-9.35691900	2.85064900
C	-3.84297100	-7.97457900	3.09644000
C	-4.40051300	-7.05189900	2.21379100
C	-6.87745000	-7.57209300	-2.06738000
C	-7.25439300	-8.69173400	-2.80598700
C	-6.94717100	-9.99326300	-2.37303400
C	-6.24564900	-10.19774400	-1.18850300
C	-3.12520200	9.73988500	-2.06820200
C	-3.90787300	10.62561400	-2.80584400

C	-5.18822700	11.00966400	-2.37107400
C	-5.71419900	10.50423000	-1.18578200
C	-6.25070600	8.85696600	1.71733900
C	-6.14661600	8.06109600	2.85442600
C	-4.98210200	7.31274800	3.09864700
C	-3.90555300	7.33496800	2.21443800
C	9.99811000	-2.16597000	-2.06819200
C	11.15627400	-1.93191100	-2.80648900
C	12.12992300	-1.01568800	-2.37245900
C	11.95630800	-0.30714600	-1.18718100
C	10.80009600	0.98317700	1.71563700
C	10.05936700	1.29232300	2.85272100
C	8.82867800	0.65898800	3.09777100
C	8.30870700	-0.28474700	2.21443500
H	0.74786300	-2.14351500	-1.58379200
H	2.96482800	-3.20156100	-1.58934800
H	4.35606800	-0.29905900	1.26117300
H	2.14061200	0.76136600	1.26167500
H	-0.40985900	-2.23489200	1.26106100
H	-2.43668500	-3.62231200	1.26110400
H	-4.25445900	-0.96483000	-1.58823200
H	-2.22917100	0.42499800	-1.58343000
H	1.48270100	1.71811000	-1.58546900
H	1.29067800	4.16687100	-1.59179000
H	-1.91682500	3.92173600	1.26080800
H	-1.72799700	1.47287900	1.26186700
H	-3.67742400	-5.12411900	-0.03102300
H	-7.95083000	-5.46826600	-0.15083400
H	-8.13687800	-2.99457000	-0.36379900
H	-6.10957000	-1.58475300	-0.32922600
H	6.27797600	-0.62132300	-0.03192800
H	8.71354400	-4.14946000	-0.15244900
H	6.66469500	-5.54774600	-0.36680500
H	4.42981900	-4.49754500	-0.33253400
H	-2.59965700	5.74571300	-0.03184000
H	-0.76357200	9.61980900	-0.15378200
H	1.47207100	8.54542100	-0.36978700
H	1.68102900	6.08507400	-0.33566200
H	-4.60882400	-10.91287000	1.53008000
H	-3.46346100	-10.04999300	3.55796800
H	-3.34938300	-7.61453600	3.99518000
H	-4.35573700	-5.98681600	2.41621100
H	-7.11065300	-6.57023200	-2.41249000
H	-7.79544400	-8.55193200	-3.73799800
H	-7.25748200	-10.84511500	-2.97142500
H	-6.00067500	-11.20433200	-0.85946700
H	-2.14132400	9.44131300	-2.41466000
H	-3.51787800	11.02435100	-3.73849400
H	-5.77204600	11.70387600	-2.96877100
H	-6.70817900	10.79482800	-0.85555800
H	-7.14757200	9.44342900	1.53515600
H	-6.96906500	8.02044300	3.56290000
H	-4.91538700	6.70535500	3.99732000
H	-3.00484900	6.76425500	2.41551300
H	9.24696200	-2.86834600	-2.41410600
H	11.30574100	-2.46935500	-3.73908900
H	13.02282200	-0.85793100	-2.97067500
H	12.70553400	0.40799500	-0.85742900
H	11.75672300	1.46580200	1.53279000
H	10.43611000	2.02512800	3.56058500
H	8.26978200	0.90590000	3.99647100
H	7.36386700	-0.77865100	2.41626500

N-Ph-o-Cb, neutral state

E_{total} = -2991.6758183 Hartree // B3LYP/6-31G(d)

C	-0.85431400	1.13124200	-0.40025100
N	0.00054500	-0.00216100	-0.42881000
C	-0.55397400	-1.30902400	-0.40092500

C	1.40947900	0.17138500	-0.40117000
C	0.01027100	-2.31502200	0.39861200
C	-0.54874400	-3.58846900	0.42240300
C	-1.69478500	-3.90289700	-0.32658500
C	-2.24901600	-2.88967900	-1.12688600
C	-1.68561600	-1.62004400	-1.17273000
C	2.24478600	-0.65409700	-1.17183400
C	3.62589300	-0.50552100	-1.12775900
C	4.22604800	0.48354900	-0.33042800
C	3.38064900	1.31925300	0.41799800
C	1.99843000	1.16504400	0.39604800
C	-0.55829500	2.26717300	-1.17160900
C	-1.37705500	3.38922700	-1.12589000
C	-2.53210200	3.41471600	-0.32627100
C	-2.83221200	2.26469300	0.42249500
C	-2.00788200	1.14455300	0.39898000
C	5.69823100	0.68514300	-0.29614800
C	-2.25853400	-5.27765500	-0.28902100
C	-3.44218200	4.58928900	-0.28993100
C	6.62288800	-0.37134700	-0.13228800
C	7.99973300	-0.11878100	-0.12941600
C	8.48775800	1.17644700	-0.28446400
C	7.58851000	2.23405900	-0.42569000
C	6.21827800	1.98550200	-0.42796200
C	-3.63638200	-5.54757200	-0.12571500
C	-4.10797100	-6.86555200	-0.11855200
C	-3.23170700	-7.93764100	-0.26891000
C	-1.86566200	-7.69020000	-0.40965300
C	-1.39389800	-6.37998300	-0.41599900
C	-2.98887000	5.91825500	-0.12717000
C	-3.89580300	6.98455800	-0.12256100
C	-5.26189900	6.75989400	-0.27456200
C	-5.72881000	5.45241300	-0.41450700
C	-4.82868600	4.38983500	-0.41861800
N	6.18900100	-1.71812400	0.05850300
N	-4.58453000	-4.49647800	0.06036200
N	-1.60518100	6.21592800	0.06054300
C	-0.85210100	5.93833600	1.20420100
C	0.45840800	6.45319900	1.03076200
C	0.49343300	7.07669000	-0.27598600
C	-0.79939100	6.91641300	-0.83946000
C	6.39179600	-2.76803500	-0.83952500
C	5.88519800	-3.96669300	-0.27280200
C	5.36450700	-3.62193800	1.03394700
C	5.57373300	-2.22915400	1.20411400
C	-5.81868000	-2.82389300	1.02747600
C	-6.37819700	-3.10837100	-0.27774400
C	-5.59479500	-4.15020600	-0.83936900
C	4.76013800	-4.35702800	2.06096700
C	4.38086500	-3.70343900	3.22986900
C	4.60389100	-2.32342900	3.38306800
C	5.20299600	-1.56834000	2.37750900
C	6.96205400	-2.74134200	-2.11550800
C	7.02838100	-3.94218400	-2.81984600
C	6.53755600	-5.14017500	-2.27233300
C	5.96502800	-5.15807000	-1.00314900
C	-7.44928700	-2.58411900	-1.01062300
C	-7.72071500	-3.09478700	-2.27731100
C	-6.92982000	-4.12237800	-2.81988800
C	-5.85732700	-4.66317900	-2.11293800
C	-4.31337300	-2.80431600	3.37627400
C	-5.39591000	-1.92061300	3.21876700
C	-6.15175700	-1.92728100	2.05000700
C	-1.23613500	5.28674900	2.37848500
C	-0.28010500	5.14489500	3.38153100
C	1.02625500	5.64146700	3.22507500
C	1.39978300	6.29690800	2.05535700
C	1.48360000	7.74126900	-1.00883800
C	1.17880200	8.22811900	-2.27731200
C	-0.10548000	8.05437400	-2.82164100

C	-1.11066500	7.39682700	-2.11473100
H	0.88117400	-2.09509200	1.00734400
H	-0.10595200	-4.34483400	1.06501800
H	-3.11564000	-3.10224200	-1.74451100
H	-2.12147400	-0.85905500	-1.81195600
H	1.80391400	-1.41367200	-1.80929000
H	4.24331000	-1.15030400	-1.74479100
H	1.37248700	1.81011000	1.00394800
H	0.31886800	2.26486700	-1.81054900
H	-1.12829700	4.24634800	-1.74323700
H	-3.70913700	2.25851300	1.06442000
H	-2.25252100	0.27988800	1.00721900
H	8.67920300	-0.95406600	0.01174200
H	9.55883600	1.35737300	-0.28234800
H	7.95227400	3.25100400	-0.54456000
H	5.52302600	2.80818800	-0.56791400
H	-5.17146100	-7.03430700	0.02218500
H	-3.61206600	-8.95511300	-0.26361000
H	-1.16794100	-8.51514900	-0.52485600
H	-0.33334500	-6.19134700	-0.55524100
H	-3.51164900	7.99057800	0.01763900
H	-5.95393200	7.59716600	-0.27104600
H	-6.79169500	5.25920600	-0.53099200
H	-5.19409900	3.37646800	-0.55758600
H	4.59407400	-5.42541200	1.94767600
H	3.91215200	-4.26327400	4.03435600
H	4.30457300	-1.83306700	4.30553100
H	5.37378600	-0.50400800	2.50019400
H	7.34397400	-1.81841200	-2.54048500
H	7.46899900	-3.94916700	-3.81319400
H	6.60533300	-6.05954800	-2.84703600
H	5.58358200	-6.08583200	-0.58421400
H	-8.06104300	-1.78709300	-0.59559900
H	-8.55034700	-2.69563300	-2.85394400
H	-7.15660900	-4.50499300	-3.81140600
H	-5.24984100	-5.45804300	-2.53413600
H	-3.73880900	-2.78627500	4.29851100
H	-5.64532200	-1.23029400	4.01974800
H	-6.99309500	-1.24875000	1.93341700
H	-2.24306800	4.90280300	2.50374100
H	-0.55288300	4.64038200	4.30459300
H	1.74746600	5.51514900	4.02769900
H	2.40784300	6.68714100	1.93963400
H	2.47885900	7.87458800	-0.59240300
H	1.93978700	8.74628500	-2.85396200
H	-0.32213200	8.43937100	-3.81450200
H	-2.10195500	7.26621000	-2.53725600
H	3.81409600	2.08296300	1.05829300
C	-4.71830700	-3.70215600	1.20197800
C	-3.96046100	-3.70636200	2.37527000
H	-3.12493900	-4.38680200	2.50141300

N-Ph-2-Th, radical cation

E_{total} = -2404.923962 Hartree // UB3LYP/6-31G(d)

C	1.01211437	-0.98410846	0.07111476
N	-0.00012629	-0.00012318	0.07181746
C	0.34592864	1.36849409	0.07107759
C	-1.35839461	-0.38470308	0.07115832
C	-0.39670824	2.29555222	0.83172165
C	-0.04982187	3.63340169	0.83305659
C	1.04084804	4.11723363	0.07022421
C	1.77125772	3.17233626	-0.68872419
C	1.44026616	1.82975608	-0.68826838
C	-2.30509420	0.33238062	-0.68813955
C	-3.63330092	-0.05222022	-0.68847739
C	-4.08639264	-1.15715396	0.07057411
C	-3.12200224	-1.85973554	0.83341283

C	-1.78993521	-1.49129423	0.83193737
C	0.86444446	-2.16249409	-0.68821369
C	1.86173108	-3.12034392	-0.68876212
C	3.04529964	-2.96014731	0.07005635
C	3.17157580	-1.77369874	0.83293081
C	2.18632625	-0.80444263	0.83170762
C	1.38508549	5.52783005	0.07597168
C	-5.48011784	-1.56431961	0.07638694
C	4.09497315	-3.96336356	0.07548131
C	0.64234133	6.59296553	0.56229684
C	1.27623326	7.84869626	0.40442106
C	2.50542509	7.74755837	-0.19961707
S	2.90531974	6.11328117	-0.58534366
C	-6.03135934	-2.73949031	0.56407339
C	-7.43573168	-2.81861153	0.40581914
C	-7.96254023	-1.70434704	-0.19990819
S	-6.74703861	-0.54142769	-0.58683498
C	5.38868718	-3.85267509	0.56206286
C	6.15956444	-5.02919751	0.40355029
C	5.45774671	-6.04292525	-0.20127899
S	3.84241681	-5.57228004	-0.58696253
H	-1.22062473	1.94948547	1.44655499
H	-0.61183574	4.31617847	1.46059828
H	2.59525194	3.50363788	-1.31310687
H	2.00201888	1.13342566	-1.30149893
H	-1.98298621	1.16698931	-1.30145854
H	-4.33223314	0.49576058	-1.31281089
H	-3.43225887	-2.68781495	1.46100742
H	-1.07825593	-2.03178339	1.44675904
H	-0.01947882	-2.30092327	-1.30140203
H	1.73665893	-3.99959098	-1.31315348
H	4.04398634	-1.62825761	1.46031137
H	2.29863215	0.08214769	1.44649094
H	-0.34216517	6.48027379	1.00171925
H	0.84212054	8.79039549	0.71987621
H	3.20130125	8.54174626	-0.43577764
H	-5.44170296	-3.53512275	1.00488374
H	-8.03431344	-3.66498083	0.72223885
H	-8.99818170	-1.49913652	-0.43673112
H	5.78304684	-2.94390091	1.00211571
H	7.19213097	-5.12402649	0.71910771
H	5.79790635	-7.04241212	-0.43806432

N-Ph-3-Th, radical cation

E_{total} = -2404.917917 hartree // B3LYP/6-31G(d)

C	1.01912747	-0.97885513	-0.01115028
N	-0.00767586	-0.00928737	0.01995663
C	0.31853969	1.36514104	0.03552285
C	-1.36087102	-0.41403731	0.03529482
C	-0.42209985	2.26599649	0.82662464
C	-0.09429834	3.61091648	0.83984167
C	0.97264633	4.12079757	0.06659068
C	1.70368569	3.20105697	-0.71945008
C	1.39101214	1.85380584	-0.73885926
C	-2.32904983	0.30129463	-0.69944863
C	-3.65204502	-0.10170647	-0.68061258
C	-4.07454427	-1.22542140	0.06571697
C	-3.09088122	-1.92527578	0.79983229
C	-1.76225782	-1.53680532	0.78661827
C	0.87735769	-2.14503721	-0.78963440
C	1.88955180	-3.08899480	-0.81794162
C	3.07842239	-2.92274615	-0.07281610
C	3.20176783	-1.74609324	0.70084678
C	2.20111016	-0.79183783	0.73503709
C	1.30261792	5.54734235	0.08103535
C	-5.47493926	-1.65284160	0.07934187
C	4.13724569	-3.93368917	-0.10291673

C	0.92385482	6.46538910	1.12481861
C	1.34769284	7.73985323	0.89752628
S	2.21117044	7.87057504	-0.60460210
C	2.01277767	6.19242127	-0.91775120
C	-6.06873720	-2.48204839	1.09698781
C	-7.38717681	-2.74230355	0.87445164
S	-7.94944912	-1.99851364	-0.59175027
C	-6.40031151	-1.31926409	-0.89559850
C	4.30112428	-4.91787176	-1.14228512
C	5.36045218	-5.74806018	-0.93213631
S	6.18807714	-5.37008681	0.54815931
C	5.10778134	-4.07407216	0.87505771
H	-1.23643822	1.89920511	1.44214262
H	-0.68193915	4.28403693	1.45460137
H	2.53921895	3.55109655	-1.31653741
H	1.95858247	1.17296597	-1.36401989
H	-2.03010254	1.15762918	-1.29424090
H	-4.37952066	0.47062251	-1.24662379
H	-3.37333917	-2.79466313	1.38354140
H	-1.03071589	-2.08311349	1.37218814
H	-0.01821393	-2.29093203	-1.38390934
H	1.75444143	-3.97927545	-1.42249613
H	4.10548768	-1.57477218	1.27625906
H	2.31556639	0.09394318	1.35047286
H	0.39092693	6.17726875	2.02332837
H	1.21772560	8.61049411	1.52591850
H	2.38978656	5.77442342	-1.84101816
H	-5.54235268	-2.83641988	1.97544647
H	-8.06906414	-3.31543360	1.48791317
H	-6.23743065	-0.74617659	-1.79799804
H	3.67701449	-4.97764482	-2.02617957
H	5.71563749	-6.55240843	-1.56193674
H	5.21434954	-3.50974852	1.79127341

N-Ph-p-Cb, radical cation

E_{total} = -2991.476981 Hartree // B3LYP/6-31G(d)

C	-1.41079438	0.11767234	-0.00247618
N	-0.00057238	0.00009020	-0.00266247
C	0.60274056	-1.27996516	-0.00234844
C	0.80634443	1.16260562	-0.00256890
C	1.75442860	-1.52901504	0.76738799
C	2.34118129	-2.78495632	0.76248368
C	1.81218626	-3.84624648	-0.00160795
C	0.65711411	-3.57906948	-0.76609194
C	0.06194239	-2.32709498	-0.77173329
C	1.98328835	1.21786510	-0.77238417
C	2.77005462	2.35919702	-0.76682505
C	2.42437046	3.49297712	-0.00194089
C	1.24099225	3.42045979	0.76251879
C	0.44654741	2.28443515	0.76746705
C	-2.20242187	-0.75465945	0.76775731
C	-3.58347209	-0.63468613	0.76275617
C	-4.23797773	0.35364976	-0.00200379
C	-3.42894051	1.21979632	-0.76702031
C	-2.04712475	1.10915700	-0.77248936
C	3.26498734	4.70322861	-0.00140971
C	2.44036432	-5.17917682	-0.00113566
C	-5.70640752	0.47626435	-0.00166441
C	4.65959835	4.62534559	-0.18837774
C	5.45661708	5.76146556	-0.18329223
C	4.88162116	7.03024400	0.00000406
C	3.49182361	7.12624194	0.18244282
C	2.70521253	5.98286845	0.18618086
C	1.67590197	-6.34832509	-0.18728962
C	2.26178162	-7.60641087	-0.18227144
C	3.64826004	-7.74226813	0.00008731
C	4.42597376	-6.58633023	0.18177400

C	3.82862204	-5.33364798	0.18557747
C	-6.33654793	1.72273880	-0.18925171
C	-7.71900592	1.84457763	-0.18436443
C	-8.53004229	0.71210723	-0.00067009
C	-7.91798604	-0.53924849	0.18242899
C	-6.53446525	-0.64844411	0.18633288
N	5.68501363	8.18658408	0.00081731
N	4.24851301	-9.01594903	0.00082576
N	-9.93318715	0.82929670	-0.00004747
C	5.63112814	9.22623735	0.94673604
C	6.59566624	10.20545842	0.60440715
C	7.26002118	9.74469627	-0.60009494
C	6.67884523	8.49958835	-0.94408754
C	5.17667576	-9.48842457	0.94624727
C	5.54290139	-10.81323833	0.60398390
C	4.81106752	-11.15885659	-0.59995689
C	4.02254552	-10.03347602	-0.94367951
C	-10.80651757	0.26295821	0.94606225
C	-12.13690368	0.60801736	0.60341151
C	-12.07020030	1.41320898	-0.60145340
C	-10.70132317	1.53278868	-0.94534775
C	4.84857774	9.34175839	2.09898544
C	5.02189150	10.47725391	2.88940465
C	5.95700957	11.46748128	2.55037764
C	6.75216009	11.33370517	1.41303814
C	8.26341787	10.28562914	-1.40750428
C	8.66681731	9.58820279	-2.54529619
C	8.06505773	8.36682281	-2.88596949
C	7.06075404	7.80761898	-2.09678318
C	-13.04049553	2.01098371	-1.40923562
C	-12.63835701	2.70868034	-2.54730279
C	-11.27973284	2.79856914	-2.88787990
C	-10.29315891	2.20914475	-2.09832616
C	-10.51517163	-0.47184055	2.09871321
C	-11.58514675	-0.88951652	2.88918649
C	-12.91033846	-0.57546419	2.54982813
C	-13.19219128	0.17940486	1.41209792
C	5.66841101	-8.86793699	2.09802227
C	6.56603379	-9.58510647	2.88801792
C	6.95651395	-10.88992379	2.54903302
C	6.44266495	-11.51221126	1.41218632
C	4.77787881	-12.29847848	-1.40709925
C	3.97145296	-12.29978565	-2.54436730
C	3.21379297	-11.16842189	-2.88480738
C	3.23157910	-10.01889121	-2.09587795
H	2.16509947	-0.74074834	1.38944660
H	3.20148122	-2.96059534	1.40047913
H	0.24512437	-4.35468703	-1.40381257
H	-0.80727206	-2.14236063	-1.39408257
H	2.25765658	0.37280892	-1.39494457
H	3.64752902	2.39022427	-1.40485403
H	0.96328011	4.25320258	1.40080318
H	-0.44124873	2.24595034	1.38981176
H	-1.72520505	-1.50414272	1.39026432
H	-4.16580369	-1.29144143	1.40116529
H	-3.89454247	1.96403599	-1.40524258
H	-1.45245865	1.76917523	-1.39516847
H	5.13597299	3.65500553	-0.28944471
H	6.53297540	5.67130254	-0.28240360
H	3.03168573	8.10341001	0.28199812
H	1.62957851	6.09063794	0.28667305
H	0.59727793	-6.27613012	-0.28762520
H	1.64577490	-8.49373147	-0.28071548
H	5.50239170	-6.67599159	0.28067987
H	4.45948900	-4.45572844	0.28545650
H	-5.73461786	2.62057305	-0.29062700
H	-8.17933139	2.82165518	-0.28391819
H	-8.53395841	-1.42643006	0.28231341
H	-6.08974426	-1.63370291	0.28730043
H	4.13831279	8.57345171	2.38354523

H	4.42307265	10.59132531	3.78832001
H	6.06800085	12.34083049	3.18589941
H	7.48847388	12.09245501	1.16336819
H	8.71762488	11.24004820	-1.15655136
H	9.44706550	9.99741704	-3.17988380
H	8.38137576	7.84629279	-3.78521139
H	6.58852123	6.87431150	-2.38259118
H	-14.09414469	1.92684109	-1.15835462
H	-13.38298232	3.17921495	-3.18218470
H	-10.98720393	3.33246999	-3.78733613
H	-9.24877951	2.26709794	-2.38409166
H	-9.49461753	-0.70226310	2.38353717
H	-11.38443501	-1.46463467	3.78840744
H	-13.72213223	-0.91603122	3.18539908
H	-14.21751120	0.43718580	1.16216551
H	5.35779264	-7.86877388	2.38250731
H	6.96458052	-9.12312970	3.78656279
H	7.65808111	-11.42218519	3.18420778
H	6.73200722	-12.52915012	1.16255895
H	5.37794324	-13.16867718	-1.15635437
H	3.93576988	-13.18026531	-3.17873881
H	2.60428154	-11.18259908	-3.78366176
H	2.65882530	-9.14361215	-2.38151476

N-Ph-m-Cb, radical cation

E_{total} = -2991.469723 Hartree // B3LYP/6-31G(d)

C	-1.18128938	0.78288443	-0.17469516
N	-0.00090035	0.00030886	-0.17476970
C	1.26703832	0.63131467	-0.17513201
C	-0.08839679	-1.41325155	-0.17419248
C	2.32230533	0.11626895	-0.94970074
C	3.56234889	0.73878685	-0.94460483
C	3.80360832	1.89412274	-0.17584264
C	2.73643611	2.39844443	0.59280017
C	1.49261953	1.78388023	0.59952326
C	0.79714037	-2.18436983	0.60079729
C	0.70773891	-3.56885011	0.59479100
C	-0.26248678	-4.24144907	-0.17344632
C	-1.14269333	-3.45537450	-0.94247302
C	-1.06217329	-2.07017733	-0.94815846
C	-1.26325368	1.95414114	-0.94944937
C	-2.42253462	2.71660092	-0.94412867
C	-3.54336365	2.34787258	-0.17482967
C	-3.44614892	1.17171011	0.59401939
C	-2.29186276	0.40202737	0.60051826
C	-0.34998409	-5.71866359	-0.17747565
C	5.12698711	2.55629011	-0.18020272
C	-4.77880310	3.16240701	-0.17925173
C	0.80862584	-6.50442661	-0.07024330
C	0.73037684	-7.90039227	-0.07536580
C	-0.51533232	-8.53314512	-0.19653112
C	-1.66857554	-7.75976723	-0.31595671
C	-1.59178894	-6.36885214	-0.30422713
C	5.22909202	3.95242094	-0.07213732
C	6.47755387	4.58187703	-0.07728394
C	7.64788784	3.81879580	-0.19932610
C	7.55379451	2.43354743	-0.31983634
C	6.31044896	1.80535278	-0.30812893
C	-6.03869819	2.55223932	-0.07141895
C	-7.20840708	3.31820920	-0.07729100
C	-7.13327593	4.71326778	-0.20001769
C	-5.88676674	5.32492312	-0.31998147
C	-4.72072641	4.56276668	-0.30736882
N	1.91008742	-8.67721093	0.03914559
N	-8.47103977	2.68529614	0.03831311
N	6.56127559	5.99179610	0.03830890
C	2.31457891	-9.68337257	-0.84883879
C	3.54410028	-10.22568315	-0.39714963

C	3.89688133	-9.51609133	0.81821372
C	2.86939363	-8.56840500	1.05550912
C	7.23086653	6.84559088	-0.84893851
C	7.08685819	8.18119108	-0.39586637
C	6.29622833	8.13125352	0.81966784
C	5.98839036	6.76755603	1.05568767
C	-9.54499886	2.83711361	-0.84947001
C	-10.62934755	2.04421425	-0.39630272
C	-10.19078793	1.38526373	0.81963595
C	-8.85618116	1.80136049	1.05587184
C	4.96363630	-9.61317139	1.71489148
C	4.98944053	-8.77750663	2.83132781
C	3.95466602	-7.85672563	3.06131172
C	2.88000972	-7.73977682	2.18107639
C	1.70661231	-10.12069057	-2.02938753
C	2.33827359	-11.13797864	-2.74287842
C	3.54748942	-11.69801148	-2.30025914
C	4.15805803	-11.24294016	-1.13150083
C	-9.62011832	3.58063160	-2.03106012
C	-10.81722563	3.54141865	-2.74403290
C	-11.90678984	2.77505820	-2.29988633
C	-11.81762316	2.02040038	-1.13009352
C	-10.80793518	0.51105178	1.71758310
C	-10.09671588	0.07209980	2.83423623
C	-8.78179572	0.50802417	3.06320658
C	-8.14348635	1.37914420	2.18168481
C	7.91308523	6.53842794	-2.02996709
C	8.47900304	7.59437854	-2.74246516
C	8.36048136	8.92123895	-2.29848332
C	7.66154595	9.22182015	-1.12929178
C	5.84796964	9.10299552	1.71755762
C	5.11164224	8.70683575	2.83393857
C	4.83080564	7.35025537	3.06264991
C	5.26574191	6.36173560	2.18115262
H	2.15522236	-0.75531703	-1.57366823
H	4.34750956	0.34594314	-1.58298775
H	2.89568702	3.26457049	1.22775741
H	0.69664484	2.17570356	1.22391749
H	1.53429467	-1.69040721	1.22495198
H	1.37836606	-4.13942263	1.22992121
H	-1.87542551	-3.93937431	-1.58057818
H	-1.73358767	-1.49010120	-1.57236316
H	-0.42520825	2.24500747	-1.57396020
H	-2.47529314	3.59284218	-1.58270890
H	-4.27565643	0.87655671	1.22923599
H	-2.23271674	-0.48303885	1.22512334
H	1.78581731	-6.03537691	-0.02656128
H	-0.57184143	-9.61642101	-0.17515803
H	-2.63571189	-8.24679810	-0.39757941
H	-2.50348144	-5.78238933	-0.36274263
H	4.33468962	4.56469652	-0.02782751
H	8.61463106	4.31081159	-0.17781227
H	8.45874015	1.83899866	-0.40227405
H	6.25772042	0.72265024	-0.36745662
H	-6.12123306	1.47149189	-0.02688865
H	-8.04300814	5.30409893	-0.17900602
H	-5.82476415	6.40590814	-0.40269404
H	-3.75688526	5.05880207	-0.36656082
H	5.75876750	-10.33477495	1.54950510
H	5.81355121	-8.84485174	3.53512093
H	3.98634546	-7.22591782	3.94504311
H	2.07447372	-7.03916159	2.37431563
H	0.78085335	-9.68213525	-2.38624844
H	1.88585165	-11.49916900	-3.66178366
H	4.01458205	-12.48964625	-2.87823339
H	5.09987521	-11.67132025	-0.80019951
H	-8.77749663	4.16241530	-2.38913255
H	-10.90407367	4.11253896	-3.66370995
H	-12.82615689	2.76570735	-2.87746141
H	-12.65949235	1.41956830	-0.79759862

H	-11.83052645	0.18315170	1.55301567
H	-10.56687627	-0.60705336	3.53901919
H	-8.25103618	0.16620285	3.94715074
H	-7.13388289	1.72665295	2.37413397
H	7.99528852	5.51773139	-2.38788589
H	9.01769108	7.38367583	-3.66167680
H	8.81305120	9.72180306	-2.87571185
H	7.56258288	10.25139100	-0.79690014
H	6.07602455	10.15240956	1.55321653
H	4.75879345	9.45370446	3.53871013
H	4.26893117	7.06175111	3.94637202
H	5.06124328	5.31372498	2.37338187

N-Ph-o-Cb, radical cation

E_{total} = -2991.460755 Hartree // B3LYP/6-31G(d)

C	0.11020235	1.41040718	-0.41737240
N	-0.00244643	0.00176645	-0.43257684
C	-1.27839701	-0.60517678	-0.41792032
C	1.16147716	-0.79943669	-0.41573710
C	-1.51096169	-1.76023862	0.35413283
C	-2.77992296	-2.31714879	0.39535878
C	-3.85694460	-1.75149253	-0.31637059
C	-3.59866973	-0.61662369	-1.11209018
C	-2.33616147	-0.04962195	-1.16401805
C	1.21142071	-1.99291507	-1.16218089
C	2.33411843	-2.80209155	-1.10834385
C	3.44426911	-2.45805653	-0.31021090
C	3.39341830	-1.24286415	0.40197506
C	2.27632769	-0.42288802	0.35860842
C	1.11969534	2.04839574	-1.16429569
C	1.26169989	3.42501476	-1.11078889
C	0.41043200	4.21600844	-0.31243868
C	-0.61804946	3.56647525	0.39949244
C	-0.77221579	2.18929162	0.35641770
C	4.64306560	-3.32374497	-0.22470064
C	-5.20645906	-2.35617085	-0.23241513
C	0.56445869	5.68657110	-0.22543093
C	4.55926712	-4.72931210	-0.08444158
C	5.72277503	-5.50660649	-0.06007500
C	6.97673625	-4.90978146	-0.16321772
C	7.07631222	-3.52083968	-0.27401212
C	5.92302406	-2.74335436	-0.29629484
C	-6.38134516	-1.58056134	-0.08943717
C	-7.63657789	-2.19895402	-0.06638576
C	-7.74748561	-3.58293925	-0.17377276
C	-6.59490660	-4.36394005	-0.28747554
C	-5.34461872	-3.75454592	-0.30824630
C	1.82507507	6.31345527	-0.08314221
C	1.91981675	7.70948703	-0.05668246
C	0.77805182	8.50003424	-0.15997922
C	-0.47596985	7.89506558	-0.27283622
C	-0.57601982	6.50781779	-0.29697493
N	3.30204813	-5.38277219	0.05923018
N	-6.31786210	-0.16549924	0.05822528
N	3.01781276	5.54854300	0.06009210
C	3.35900340	4.73990855	1.15349185
C	4.66259599	4.22103595	0.95069602
C	5.13759069	4.75353745	-0.31160825
C	4.10329368	5.57673957	-0.82475288
C	2.78465967	-6.33692153	-0.82608161
C	1.55761862	-6.82627247	-0.31059843
C	1.33524884	-6.15222930	0.95386299
C	2.43393334	-5.27936573	1.15540148
C	-5.99857417	1.92003438	0.95790117
C	-6.69422354	2.06820491	-0.30573245
C	-6.88537258	0.76233902	-0.82433593
C	0.32814518	-6.22506484	1.92249820

C	0.43150793	-5.43971801	3.06865206
C	1.53648144	-4.59198400	3.25856971
C	2.55286180	-4.50135172	2.30887410
C	3.29396468	-6.76843001	-2.05443990
C	2.55813808	-7.71925961	-2.75944097
C	1.34498478	-8.22254554	-2.25965603
C	0.83868141	-7.77915703	-1.03965725
C	-7.15969637	3.16943828	-1.03169054
C	-7.79803892	2.95617405	-2.25169019
C	-7.97011439	1.65529137	-2.75460359
C	-7.51481817	0.54054527	-2.05276334
C	-4.74773112	0.95888310	3.25963956
C	-4.92820685	2.34031034	3.07317718
C	-5.55685007	2.82586620	1.92856071
C	2.62430312	4.45221889	2.30564623
C	3.20747914	3.61146746	3.25233246
C	4.49236121	3.07458511	3.06102471
C	5.22587058	3.37972052	1.91648626
C	6.32224485	4.60607741	-1.04052000
C	6.45592873	5.27017640	-2.25805628
C	5.41634706	6.07427133	-2.75561171
C	4.22512378	6.23746970	-2.05072197
H	-0.71039628	-2.18808707	0.94813662
H	-2.95361847	-3.18026863	1.03042556
H	-4.39313442	-0.18730015	-1.71168789
H	-2.15289657	0.81157484	-1.79752855
H	0.37549351	-2.26493361	-1.79766004
H	2.36136462	-3.70441185	-1.70839566
H	2.24506493	0.48437965	0.95249722
H	1.77236677	1.45898993	-1.79929334
H	2.03047962	3.89819383	-1.71084982
H	-1.27702493	4.14839126	1.03633734
H	-1.54308363	1.71005691	0.95049857
H	5.62976260	-6.58098580	0.06364440
H	7.87134928	-5.52465599	-0.13894894
H	8.04983886	-3.04614890	-0.35117446
H	6.00418159	-1.66670270	-0.41418826
H	-8.52012212	-1.58115257	0.05976123
H	-8.72753547	-4.04979034	-0.15050898
H	-6.67120931	-5.44409108	-0.36802958
H	-4.45318201	-4.36329006	-0.42836767
H	2.89774837	8.16354672	0.06871653
H	0.86592207	9.58197935	-0.13417205
H	-1.37226308	8.50311865	-0.35007441
H	-1.55005857	6.04233792	-0.41632301
H	-0.51619490	-6.89607804	1.78848800
H	-0.33886094	-5.49509355	3.83233041
H	1.60854431	-4.00281026	4.16852592
H	3.41025796	-3.85584563	2.46817925
H	4.23176769	-6.38503390	-2.44349841
H	2.93330022	-8.07780556	-3.71357800
H	0.79803800	-8.96589104	-2.83181902
H	-0.10079958	-8.17080693	-0.65908108
H	-7.02798098	4.17781033	-0.64870871
H	-8.16815379	3.80322176	-2.82143494
H	-8.46905885	1.51242006	-3.70871171
H	-7.65266959	-0.46224282	-2.44421919
H	-4.27334449	0.59923538	4.16845819
H	-4.58999626	3.03297898	3.83839726
H	-5.71502354	3.89305166	1.79730835
H	1.63815237	4.87514431	2.46632017
H	2.65994205	3.37779717	4.16114933
H	4.92291175	2.43079045	3.82253830
H	6.22796526	2.98129578	1.78157249
H	7.12888317	3.98425936	-0.66168320
H	7.37315557	5.16726868	-2.83006075
H	5.54145647	6.58139639	-3.70790035
H	3.42636725	6.86182223	-2.43800940
H	4.22628455	-0.96132930	1.03877965
C	-5.79309724	0.53141985	1.15589413

C	-5.17880878	0.03605621	2.30794071
H	-5.04950085	-1.02971583	2.46473554